https://doi.org/10.5194/bg-2020-206
Preprint. Discussion started: 30 June 2020

Biogeosciences Discussions

Monsoonal forcing controlled cold water coral growth off south-eastern Brazil during the past 160 kyrs

André Bahr[1], Monika Doubrawa[1,2], Jürgen Titschack[3,4], Gregor Austermann[1], Dirk Nürnberg[5], Ana Luiza Albuquerque[6], Oliver Friedrich[1], Jacek Raddatz[7]

[1]Institute of Earth Sciences, Heidelberg University, Im Neuenheimer Feld 234, 69120 Heidelberg, Germany
[2]Earth and Environmental Sciences,KU Leuven, Celestijnenlaan 200e, 3001 Leuven, Belgium
[3]MARUM – Center for Marine Environmental Sciences, University of Bremen, Leobener Str. 8, 28359 Bremen, Germany
[4]Senckenberg am Meer, Marine Research Department, 26382 Wilhelmshaven, Germany
[5]GEOMAR Helmholtz Centre for Ocean Research, Wischhofstraße 1-3, 24148 Kiel, Germany
[6]Departamento de Geoquímica, Universidade Federal Fluminense, Outeiro São João Baptista s/n. – Centro, Niterói, RJ, Brazil
[7]Institute of Geosciences, Goethe University, Frankfurt, Altenhöferallee 1, 60438 Frankfurt am Main, Germany

Correspondence to: André Bahr (andre.bahr@geow.uni-heidelberg.de)

Abstract. Cold-water corals (CWC) constitute important deep-water ecosystems that are increasingly under environmental pressure due to ocean acidification and global warming. The sensitivity of these deep-water ecosystems to environmental change is demonstrated by abundant paleo-records drilled through CWC mounds that reveal a characteristic alteration between rapid formation and dormant or erosive phases. Previous studies have identified several parameters such as food supply, oxygenation, and carbon saturation state of bottom water as central for driving or inhibiting CWC growth, yet there is still a large uncertainty about the relative importance of the different environmental parameters. To advance this debate we have performed a multi-proxy study on a sediment core retrieved from the 25 m high Bowie Mound, located in 866 m water depth on the continental slope off south-eastern Brazil, a structure built up mainly by the CWC *Solenosmilia variabilis*. Our results indicate a multi-factorial control on CWC growth and mound formation at Bowie Mound during the past ~160 kyrs, which reveals distinct formation pulses during glacial high northern latitude cold events (Heinrich Stadials, HS) largely associated with anomalous continental wet periods. The ensuing enhanced run-off elevated the terrigenous nutrient and organic matter supply to the continental margin, and might have boosted marine productivity. The dispersal of food particles towards the CWC colonies during HS was facilitated by the highly dynamic hydraulic conditions along the continental slope that prevailed throughout glacial periods. These conditions caused the emplacement of a pronounced nepheloid layer above Bowie Mound aiding the concentration and along-slope dispersal of organic matter. Our study thus demonstrates a yet unrecognized impact of continental climate variability on a highly vulnerable deep-marine ecosystem.

https://doi.org/10.5194/bg-2020-206
Preprint. Discussion started: 30 June 2020

1 Introduction

Cold-water corals (CWC) are hotspots of biodiversity in the deep-sea (Roberts and Cairns, 2014), important constituents of the deep water carbon cycle (Titschack et al., 2009; White et al., 2012; Cathalot et al., 2015; Titschack et al., 2015, 2016), and potent bio-engineers due to their sediment baffling capacity that allows for enormous sediment accumulation rates of up to 1500 cm/kyr during maximum CWC mound formation phases (Titschack et al., 2015; Wienberg and Titschack, 2017). Yet the fate of CWC reefs and associated ecosystems under global climate change is poorly constraint, because the factors driving or inhibiting their formation as well as potential thresholds in their resilience to environmental change are still under debate (Hebbeln et al., 2019; Raddatz and Rüggeberg, 2019). Geological records reveal that coral mounds typically exhibit distinct phases of formation, often intercalated by intermitted periods of non-deposition and/or potentially erosion, pointing at a high sensitivity of CWCs to changing boundary conditions (e.g., Rüggeberg et al., 2005; Kano et al., 2007; Frank et al., 2011; Raddatz et al., 2014, 2016; Wienberg and Titschack, 2017; Wienberg et al., 2018).

The most common framework-forming CWC comprise preferences of *S. variabilis*, the dominant framework-building CWC discussed in this study, are still pending. Changes the species *Lophelia pertusa* (recently assigned to the genus *Desmophyllum* by Addamo et la., 2016), *Macropora oculata*, *Solenosmilia variabilis*, *Bathelia candida*, and *Enallopsammia profunda* (e.g., Mangini et al., 2010; Frank et al., 2011; Muñoz et al., 2012; Hebbeln et al., 2014; Raddatz et al., 2020). Field and laboratory studies of *L. pertusa*, the most intensively investigated species, suggest that scleractinian CWC are non-specialists regarding food sources, which may range from POC to DOC (Kiriakoulakis et al., 2005; Duineveld et al., 2007; Gori et al., 2014; van Oevelen et al., 2016), algae, bacteria, and zooplankton (Gori et al., 2014; Mueller et al., 2014; Wienberg and Titschack, 2017). Note, however, that similar studies in the feeding in the properties and spatial configuration of ambient intermediate- or deep-water masses might have a strong impact on CWC as they alter the dissolved oxygen concentration and also the seawater parameters pH, alkalinity and carbonate-ion concentration. All affect the capacity of CWC to build their aragonitic framework (e.g., Form and Riebesell, 2012; Maier et al., 2012; Lunden et al., 2014; Hennige et al., 2015; Büscher et al., 2017). Spatial fluctuations of intermediate- to deep-water masses further influence the depth and strength of pycnoclines, which are thought to play an important role for the concentration and dispersal of nutrients and food utilized by CWC (Frederiksen et al., 1992; Duineveld et al., 2007; Mienis et al., 2007; Rüggeberg et al., 2016). Aside of processes directly affecting the water-mass properties bathing CWC, several studies also point at the importance of surface productivity in providing food that is transported to the deep ocean (Davies et al., 2009; Soetaert et al., 2016). The role of adjacent continents via the input of terrestrial nutrients and POC is still a matter of debate considering the proximity of CWC situated on the continental slope to land.

To systematically test the relative importance of the diverse factors potentially influencing CWC growth and mound formation, we investigated the response of CWC at Bowie Mound, a coral-bearing mound in the Campos Basin on the continental slope offshore SE Brazil (Bahr et al., 2016; Raddatz et al., 2020) to changes in paleoenvironmental conditions. CWC-bearing mounds off Brazil were first reported by Viana et al. (1998) and Sumida et al. (2004) along the continental slope at intermediate water depths between 500 to 1000 m within the Antarctic Intermediate Water (AAIW). At Bowie Mound, the dominating species is *S. variabilis*, which is adopted to colder (as low as 3-4°C; Fallon

https://doi.org/10.5194/bg-2020-206
Preprint. Discussion started: 30 June 2020

et al., 2014; Flögel et al., 2014; Gammon et al., 2018) and less aragonite saturated waters than mounds formed by *L. pertusa* (Thresher et al., 2011; Flögel et al., 2014; Bostock et al., 2015; Gammon et al., 2018).

The selected location at Bowie Mound is ideally suited to test for a variety of external factors potentially driving CWC growth dynamics as it is situated at the interface of distinctly different water masses (cf. Section 2) and is strongly influenced by terrigenous input from land and the broad shelf off Cabo Frio with intense seasonal upwelling. This setting allows us to test the relative importance of different factors that are potentially crucial for the CWC growth at Bowie Mound, in particular (i) intermediate water-mass variability and its impact on nutrient availability and local hydrodynamics as well as (ii) variations in nutrients and organic matter derived from upwelling and terrestrial input in the context of global climatic changes. Our unique set of multi-proxy data combined with Th/U-dated CWC for the first time demonstrates that an invigorated continental hydroclimate played a so far underestimated role in triggering CWC growth at the SE Brazilian margin – a scenario that is likely affecting CWC-mounds worldwide.

2 Hydrological, climatological and geological setting

The (sub)surface circulation in the western Tropical South Atlantic at the Campos Basin off southeast Brazil is dominated by the southward flowing, warm Brazil Current (BC; Fig. 1). The BC forms the western portion of the anticyclonic subtropical gyre (Stramma and England, 1999), which is characterized by high evaporation rates that lead to the formation of the Salinity Maximum Water (SMW, 24ºC, σ_θ ~ 25.2) occupying the upper 200 m of the water column. The interaction of the BC with the coastal hydrographic system promotes subsurface upwelling of South Atlantic Central Water (SACW) on the shelf edge and on the shelf (Roughan and Middleton, 2002; Aguiar et al., 2014). Upwelling is particularly strong during austral spring and summer when northeasterly winds generating upward Ekman pumping on the mid shelf (Castelao and Barth, 2006; Castelao, 2012), which fuels productivity due to the subsurface encroachment of nutrient-rich SACW. Below the SMW, the SACW is found until 500 m water depth, characterized by decreasing temperatures and salinities (20ºC, 36.0 psu to 5ºC, 34.3 psu; Fig. 1) (Raddatz et al., 2020) owing to its formation in the southwest Atlantic and the South Indian Ocean (Sverdrup et al., 1942; Stramma and England, 1999). The SACW is underlain by the Antarctic Intermediate Water (AAIW; 34.3 PSU, ~4°C) (Fig. 1). North Atlantic Deep Water (NADW) is found below 1100 m water depth with higher oxygen concentrations and salinities compared to AAIW (Mémery et al., 2000). Below ~2500 m the Antarctic Bottom Water (AABW) constitutes the deepest and most dense water mass (Stramma and England, 1999) in this region.

The interaction between the north- or southward-directed flow of the different water masses with the morphology of the slope at Campos Basin causes the formation of strong geostrophic currents (Viana and Faugères, 1998; Viana et al., 1998; Viana, 2001). These are responsible for enhanced sediment focusing leading to the formation of drift bodies, while internal waves at the boundary between different water masses create wide-spread erosional surfaces (Viana et al., 1998, 2001). Bowie Mound itself has a total elevation of 25 m and situates within a field of mound-like structures, which are at present barren of living CWC colonies (Bahr et al., 2016). With a water depth of 866 m, it lies within the core of the AAIW. Hence, it can be expected that changes in the nutrient inventory of the AAIW (Poggemann et al., 2017) and/or displacement of the intermediate water mass may have had a direct impact on the hydrodynamic conditions at Bowie Mound.

https://doi.org/10.5194/bg-2020-206
Preprint. Discussion started: 30 June 2020

The Campos Basin receives freshwater and sediment input primarily from the Paraíba do Sul River, which delivers between 180 to 4400 $m^3 s^{-1}$ water (Carvalho et al., 2002) and 30 t yr^{-1} of sediment load (Jennerjahn et al., 2010). Most precipitation in the hinterland of the Paraíba do Sul River occurs during austral summer, when strong atmospheric convection forms the South Atlantic Convergence Zone, an elongated band of heavy precipitation that reaches from central Amazonia into the tropical South Atlantic (Carvalho et al., 2004; Marengo et al., 2012) (Fig. 1).

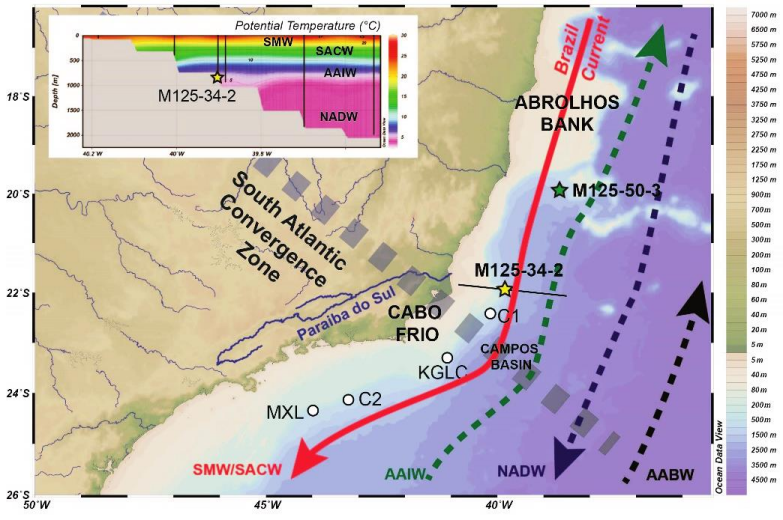

Fig. 1 Location of core M125-34-2 (yellow star) on Bowie Mound, reference core M125-50-3 (green star) and other CWC records published in Mangini et al. (2010) and Ruckelshausen (2013) (white dots). Major surface (red line), intermediate (green) and deep-water circulation features (blue) and water masses are indicated as well as the approximate location of the South Atlantic Convergence Zone (stippled line) as the main atmospheric feature. Inset shows a hydrographic section crossing the location of Bowie Mound core M125-34-2 with potential temperatures as measured via CTD (black lines) during R/V METEOR Expedition M125 (Bahr et al., 2016; Raddatz et al., 2020); the location of the hydrographic section is indicated by a black line in the map. Figure modified after Raddatz et al. (2020). AABW – Antarctic Bottom Water, AAIW – Antarctic Intermediate Water, NADW – North Atlantic Deep Water, SACW – South Atlantic Central Water, SMW – Salinity Maximum Water.

3 Material and Methods

3.1 Material

Gravity core M125-34-2 was retrieved during R/V METEOR cruise M125 from the top of the 25 m high Bowie Mound in 866 m water depth at 21°56.957'S and 39°53.117'W (exact positioning was secured by the Ultra-Short-Baseline system POSIDONIA; Fig. 1, Bahr et al., 2017). The core was cut into 1 m segments onboard and stored unopened at -20°C. After CT-scanning, the core was opened in frozen state (for details on the CT-scanning cf. Skornitzke et al., 2019; Raddatz et al., 2020). Discrete samples for X-ray Diffractometry (XRD), grain-size analyses, C and N content, and stable carbon and oxygen isotope analyses of foraminifera and organic matter were taken from the sediment matrix

https://doi.org/10.5194/bg-2020-206
Preprint. Discussion started: 30 June 2020

avoiding the sampling of coral fragments. X-ray Fluorescence (XRF) scanning was performed on the archive halve, avoiding coral segments when defining the sampling path of the detector.

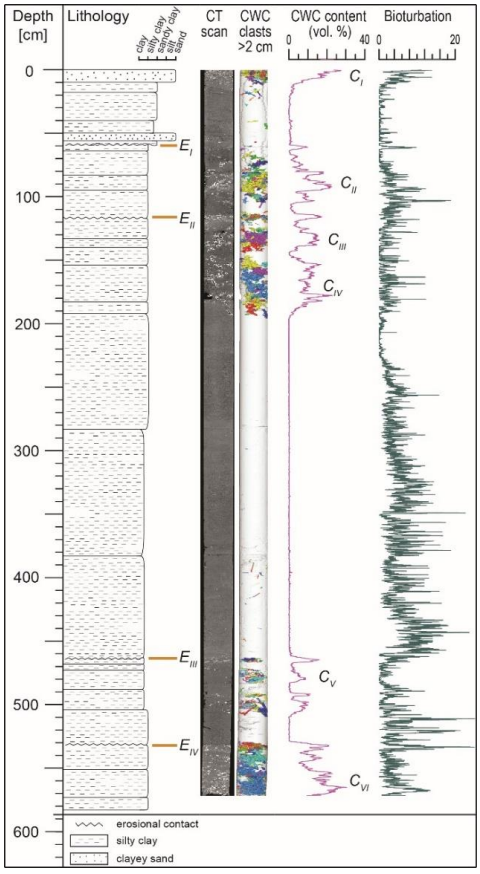

Fig. 2. Lithological log of Core M125-34-2 (21°56.957'S, 39°53.117'W, 866 m water depth) including CT-scanning image and CWC clasts >2 cm, CWC content and bioturbation index. Erosional surfaces E_I–E_{IV} are indicated as well as CWC-bearing intervals C_I–C_{VI} after Raddatz et al. (2020).

The core M125-34-2 (Fig. 2) consists of moderately to strongly bioturbated olive grey to dark grey, silty clayey sand with an alteration of coral-bearing and coral-free zones (Raddatz et al., 2020). The sediments are rich in micro- and macrofossils including pteropods, bivalves as well as benthic and planktonic foraminifers. Six intervals (C_I–C_{VI}) with particularly high coral contents of up to 31 vol.% were identified within the core located between 0–13 cm, 80–105 cm, 131.5–138 cm, 157–190 cm, 479.5–480.5 cm, and 549.5–568 cm (Raddatz et al., 2020) (Fig. 2). Coral-bearing intervals are characterized by the presence of *S. variabilis* and to a minor degree *M. oculata* as the major macrofossils (clast length >2 cm). Visual inspection and CT imaging (Appendix Figures A-F) reveal four prominent erosive surfaces (E_I–E_{IV}) with abundant coral fragments and shell debris at 58 cm, 117 cm, 465 cm, and 532 cm (Fig. 2).

For constraining the chronostratigraphy of core M125-34-2 and to assess the intermediate-water variability, adjacent core M125-50-3 (19°56.957'S; 38°35.979'W; 904 m water depth; Fig. 1) was sampled in 10 cm intervals for $\delta^{18}O$ analyses. Core M125-50-3 is barren of CWC and consists of bioturbated, greenish-grey hemipelagic mud with darker

https://doi.org/10.5194/bg-2020-206
Preprint. Discussion started: 30 June 2020

and lighter intervals. Two sandy, foraminifera-rich layers at 1226 and 1230 cm might point at periods of condensed sedimentation, otherwise no unconformities or erosive surfaces could be identified.

150

3.2 Quantitative interpretation of CT-scanning data

Prior to opening, the sediment core sections were scanned with a SOMATOM Definition Flash computer tomograph at the Clinic of Diagnostic and Interventional Radiology (DIR) of Heidelberg University Hospital, Heidelberg, Germany, with 140 kVp tube potential and 570 mAs tube current – time product with a pitch of 0.4 (for details see
155 Skornitzke et al. 2019). The raw data with a resolution of 0.5 mm in z-orientation and 0.3 mm in xy-orientation was reconstructed iteratively (ADMIRE, Siemens Healthineers) using a sharp kernel (I70 h level 3) to an isotropic voxel size of 0.35 mm. Further data processing was carried out with the ZIB edition of the Amira software (Stalling et al. 2005; http://amira.zib.de). Within Amira, the core sections were virtually reunited and the core liner and marginal coring artefacts were removed (~2 mm of the core rim). Furthermore, coral clasts were segmented and separated with
160 the ContourTreeSegmentation module (threshold: 1400; persistence value: 1150), quantified and macrofossils >2 cm were visualized as surfaces in 3D following the methodology of Titschack et al. (2015). As an index for bioturbation, we determined the standard deviation of the matrix sediment X-Ray attenuation within each XY-oriented CT slice. The matrix sediment was segmented by selecting the data volume surrounding the corals, removing areas with values <500 HU (considered to represent air and water) and reducing the remaining segmented volume by three voxels to
165 avoid marginal artefacts in the x-ray attenuation caused for example by the resolution depending averaging effect.

3.3 X-Ray fluorescence (XRF) scanning

XRF core scanning was performed on the archive halve of the split core. All segments of core M125-34-2 were scanned at the Heidelberg University, using an Avaatech 4th generation XRF Core Scanner. XRF core scanner data were
170 collected every 1 cm down-core. The split core surface was cleaned and covered with a 4 micron thin SPEXCerti Prep Ultralene1 foil to avoid contamination of the XRF measurement unit. Core intervals with very abundant corals had to be skipped to avoid damaging the foil covering the detector through sharp and rigid edges of coral fragments. Data were collected in two separate runs using generator settings of 10 and 30 kV and currents of 0.2 and 1.0 mA respectively. Sampling time was set to 20 seconds per measurement. To counteract artifacts derived from variations in
175 sediment porosity, water content and surface roughness, element counts were normalized by dividing the value of the component (C) by the sum of the counts for each depth (Bahr et al., 2014).

3.4 X-Ray diffractometry (XRD)

About 9 g of wet material was dried in an oven at 40°C and subsequently milled in a ball mill (Pulverisette, FRITSCH),
180 with 300 cycles per sec for 3 minutes to obtain a powder with a grain size of 1-3 micrometres. The XRD measurements were done at the Heidelberg University, Department of Geosciences, using a Bruker, D8 ADVANCE Eco diffractometer (40 kV, 25mA) with a Cu Kα diode. The samples were measured in rotating, circular, synthetic sample holders. An angular range of 2θ from 5° to 70° was measured with a step size of 0.02 increments (3338 steps per sample) for 1 sec per step. Peak positions and intensity of data was analyzed with Diffract Suite EVA (Bruker

https://doi.org/10.5194/bg-2020-206
Preprint. Discussion started: 30 June 2020

Software). For quantitative phase analysis the Rietveld refinement program DIFFRAC.TOPAS (Bruker Software) was used.

3.5 Grain-size analysis (Sortable Silt, $\overline{SS}$)

The preparation of the samples for the $\overline{SS}$ analyses followed Bianchi et al. (2001) and Stuut et al. (2002). Wet samples with a weight between 0.3 and 1 g were dried over night at 40 °C. Macroscopically visible coral fragments were removed. After weighting the dry samples, 10 ml of 30 % H_2O_2 were added to each sample to dissolve the organic material under sub-boiling conditions on a heating plate until the reaction ceased. To remove carbonates, 5 ml HCl (10 %) were added to each sample under sub-boiling conditions for at least 10 minutes until end of the reaction. Samples were washed through standard sieves (63 µm mesh size) to remove the sand and coarser fraction. The fraction >63 µm was dried at 40°C and weighted. The material <63 µm was transferred into 1 L beakers, filled until capacity with demineralized water. After a settling period of at least 8 hours (h), the supernatant water was decanted, and the sample transferred into a 200 mL beaker, topped with demineralized water and settled for 8 h. After decanting supernatant water the sample was transferred into a 50 mL plastic beaker, put into an ultrasonic bath to disintegrate aggregated sediment particles. Afterwards, 35 ml Na-Pyrophosphate were added to prevent particles from forming new aggregates and 2 ml isopropyl alcohol to keep the formation of air bubbles in the liquid to a minimum. Samples were measured with a Laser Particle Sizer (LPS) ANALYSETTE 22 by FRITSCH™ in wet dispersion covering the range 0.08-2000 µm with 99 size classes. For analysis of the raw data the software MaScontrol (FRITSCH™) was used applying a Fraunhofer model. Results are derived from a total of five analytical runs à 100 scans per sample. Up to seven replicate samples were performed for each depth to minimize the natural variability of the samples. The high number of replicates resulted from a relatively large inter-sample variability that is likely caused by the high amount of mica flakes present in the sediment distorting the laser beam. We nevertheless consider the results retrieved via the ANALYSETTE 22 as reliable (for an in-depth discussion see Jonkers et al., 2009).

3.6 Carbon and nitrogen content

Sediment samples were homogenized with a mortar and pestle and then weighted (0.5 mg for each analyses). The total organic carbon (TOC) and inorganic carbon (TIC, together TC) content was analyzed with a LECO RC-412 (Institute of Geoscience, Goethe University Frankfurt). The reproducibility of the replicate analyses was < ± 0.1 %. The total nitrogen (TN) content was analysed with a LECO TruSpec Macro (Institute of Geoscience, Goethe University Frankfurt).

3.7 Stable oxygen and carbon analysis

3.7.1 Stable isotope analysis of foraminiferal calcite

For stable isotope analyses of core M125-34-2, samples were taken at 5–10 cm intervals, wet-sieved (>63 µm) and dried afterwards. For each sample 1–3 tests of *Uvigerina* spp. or *Planulina wuellerstorfi* were selected from the size fraction >125 µm, depending on availability. Stable carbon and oxygen isotope ratios were measured on a Thermo Fischer MAT 253 Plus IRMS gas isotope ratio mass spectrometer with coupled Kiel IV automated carbonate

https://doi.org/10.5194/bg-2020-206
Preprint. Discussion started: 30 June 2020

preparation device at the Institute of Earth Sciences, Heidelberg University. The instrument was calibrated using the in-house standard (Solnhofen limestone), itself calibrated against the IAEA-603; values are reported versus the VPDB (Vienna Peedee Belemnite) standard. Standard deviations derived from repeated measurements of the internal standard are ±0.06 ‰ for $\delta^{18}O$ and ±0.03 % for $\delta^{13}C$.

The ~13 m long core M125-50-3 was sampled each ~10 cm for benthic foraminiferal isotope studies. The samples were freeze-dried and washed through a >63 µm sieve to separate the coarse fraction from the fine fractions. Specimens of the benthic genera *Uvigerina* spp. were hand-picked from the size fraction 315–400 µm. Stable oxygen ($\delta^{18}O$) isotope analyses were performed on a ThermoScientific MAT 253 mass spectrometer with an automated Kiel IV Carbonate Preparation Device at GEOMAR. The isotope values are calibrated versus the NBS19 (National Bureau of Standards) carbonate standard and the in-house "Standard Bremen" (Solnhofen limestone). Isotope values presented in the delta-notation are reported in permil (‰) relative to the VPDB scale. The analytic error is ±0.06‰ for $\delta^{18}O$ and ±0.03‰ for $\delta^{13}C$.

3.7.2 Stable isotope analysis of organic matter

Previously homogenized samples were decarbonized with 10 % HCl to remove all inorganic carbon. Afterwards, the samples were centrifuged and washed several times with deionized water in order to remove residual HCl. The samples were then dried in an oven at 50 °C. Subsequent analyses of the carbon isotopic composition of organic carbon ($\delta^{13}C_{org}$) was performed by a Flash Elemental Analyzer 1112, connected to the continuous flow inlet system of a MAT 253 gas source mass spectrometer (Institute of Geosciences, Goethe University Frankfurt). Samples and standards both reproduced within ±0.2‰ and are reported relative to VPDB standard.

3.7 Statistical analysis

Correlation coefficients and associated p-values were calculated using the Monte-Carlo-based SurrogateCorr function implemented in the astrochron package in R (Meyers, 2014) with 1000 iterations. This method has been particularly developed to assess the correlation of parameters sampled on different down-core resolutions (e.g. XRF scanning data *vs*. discrete grain size measurements) (Meyers, 2014).

Discriminant analysis was performed with the program PAST (v3.15) (Hammer et al., 2001). Prior to analysis, the data was detrended and normalized to mean and standard deviation.

4. Age model refinement

The age model of core M125-34-2 used in this study represents a refined version of the stratigraphy published in Raddatz et al. (2020), which is based on $^{230}Th/U$ dates of CWCs. The six coral-bearing intervals, as described in Section 3.1, exhibited a mean accumulation rate of 30 cm kyr^{-1} with an overall range from 2 cm kyr^{-1} (C_V) to 80 cm kyr^{-1} (C_{III}) (Raddatz et al., 2020).

To better constrain the age of CWC-barren intervals and evaluate the chronostratigraphic duration of potential hiatuses, we compared the $\delta^{18}O$ record of Core M125-34-2 with the benthic isotope record of adjacent core M125-50-3. The clear glacial-interglacial pattern of $\delta^{18}O_{Uvi}$ in Core M125-50-3 allows to construct a robust age model for this site by

https://doi.org/10.5194/bg-2020-206
Preprint. Discussion started: 30 June 2020


Biogeosciences Discussions Open Access EGU

tuning its benthic isotope record to the LR04 benthic stack (Lisiecki and Raymo, 2005), indicating that it reaches down to ~135 ka (Fig. 3). Its stratigraphic range is thus only slightly shorter than the one of M125-34-2 (158 ka based on Th/U dates) and therefore suitable as an off-mound reference site. As both cores are situated in similar water depths and are thus bathed by the same water mass (today the AAIW, see Section 2), we expect the respective $\delta^{18}O$ values not only to follow a common glacial/interglacial pattern but also to be comparable in their absolute values, allowing to further constrain the chronostratigraphy of M125-34-2.

As neither shallow infaunal *Uvigerina* spp. and epibenthic *P. wuellerstorfi* were consistently present throughout core M125-34, we generated a spliced record of both species. For the $\delta^{18}O$ splice we corrected values of *P. wuellerstorfi* by adding the correction factor of +0.47 ‰ according to Marchitto et al. (2014). The resultant combined $\delta^{18}O$ record of M125-34 exhibits a considerable scatter in lithological Unit 1 including relatively depleted $\delta^{18}O_{cib}$ values as low as 2.5 ‰ (Fig. 3), which puts this unit into a transitional phase between glacial and interglacial $\delta^{18}O$ levels. Neither $\delta^{18}O$ values nor absolute dating supports the preservation of Holocene deposits at the top of the gravity core. A deglacial age for the deposition of Unit 1 is further corroborated by Th/U dates of 13.7 to 14.3 ka, respectively. Unit 2 has slightly heavier $\delta^{18}O$ values than Unit 2 and Th/U dates clustering around 16.5 ka, which indicates a post-LGM deposition. The existing Th/U dates suggest that the hiatus represented by the erosive unconformity between Units 1 and 2 is most likely shorter than 2 kyr. Unit 3 on the other hand has relatively uniform $\delta^{18}O$ values that cluster around 4.3 ‰ ($\delta^{18}O_{Uvi}$) and 3.4 ‰ ($\delta^{18}O_{cib}$), respectively, which matches M125-50-3 $\delta^{18}O_{uvi}$ values during MIS 2 to 4. The age of the top of Unit 3 is relatively well defined by Th/U dates of 34 ka and older while its base lacks any absolute dating. As values of $\delta^{18}O_{uvi}$ of Unit 3 are more depleted than MIS 2 values but less than MIS 5 samples of reference site M125-50-3, we infer that lithological Unit 3 was most likely deposited during MIS 3 and potentially MIS 4 but did not reach into MIS 5. It hence appears that MIS 2 deposits are not present in core M125-34-2, either due to non-deposition or subsequent erosion (note the prominent erosive surface between Units 2 and 3). This age assignment would also imply that the CWC-free portion of Unit 3 from 200 to 465 cm has been deposited within a short period of approximately 8 kyr (62.20 ka as the oldest Th/U dates and ~70 ka as the MIS 4/5 boundary). This would yield a sedimentation rate of 33 cm kyr^{-1}, which is typical for contouritic sediments as common at the south-eastern Brazilian margin (Viana et al., 1998; Hernández-Molina et al., 2014; Rebesco et al., 2014). Unit 4 has distinctively more depleted $\delta^{18}O_{uvi}$ values in the range of MIS 5a–d values in reference core M125-50-3, but less depleted as those of MIS 5e. Th/U dates of ~107 ka of CWC at the top of Unit 4 support a deposition of this Unit in MIS 5d and further indicate a prolonged interval of non-deposition or erosion leading to the absence of MIS 5a-c in core 125-34-2. As $\delta^{18}O$ values of Unit 5 are again on glacial levels, this unit can be assigned to MIS 6 in line with Th/U dates of 152.6–158.4 ka. Hence the penultimate interglacial MIS 5e is likely not recovered and falls into the hiatus between Units 4 and 5. In summary, deposition at Bowie Mound core M125-34-2 appears to be focused on glacial intervals of intermediate ice volume, such as MIS 3, contrary to the reduced presence in interglacial deposits.

The erosive horizons present in core M125-34-2 provide evidence for extreme variability in the hydrological regime at the south-eastern Brazilian Margin (Viana and Faugères, 1998; Viana et al., 1998; Viana, 2001), produced by winnowing due to strong current activity and internal waves. While winnowing has the capacity to remove the sediment matrix leading to lag deposits, it is rather unlikely that it would also remove coral fragments. Hence, it is feasible to

https://doi.org/10.5194/bg-2020-206
Preprint. Discussion started: 30 June 2020

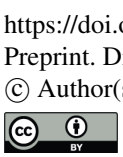

assume that the dated intervals of CWC presence represent the complete sequence of CWC presence at this part of Bowie Mound.

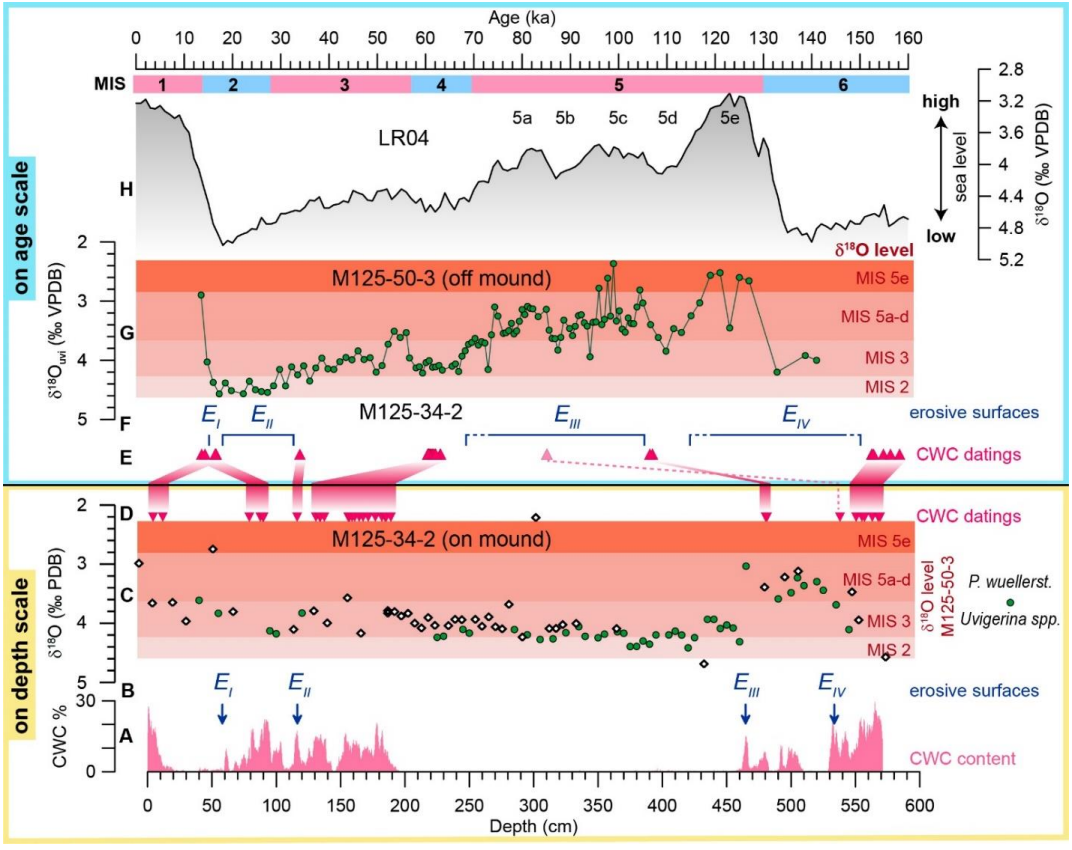

300 **Fig. 3** Refined age model of Core M125-34-2 from Bowie Mound. Lower panel displays data from M125-34-2 on depth scale, comprising (A) CWC abundances (%) based on CT-scanning; blue arrows denote erosive horizons (hiatuses); (B) erosive horizons E_I–E_{IV} (cf. Fig. 2); (C) benthic $\delta^{18}O$ data from *Uvigerina* spp. (green dots) and *P. wuellerstorfi* (white diamonds; elevated by +0.47 to adjust for the interspecies offset to *Uvigerina* spp. (Marchitto et al., 2014)); red horizontal shadings indicate reference $\delta^{18}O$ levels for the respective Marine Isotope Stages (MIS) taken
305 from off-mound core M125-50-3 (see panel G); (D) red triangles mark Th/U datings. The upper panel displays data in the time domain, with (E) Th/U dates of M125-34-2; (F) the inferred duration of hiatuses reflected by erosive horizons E_I–E_{IV} of core M125-34-2; (G) the $\delta^{18}O$ record on *Uvigerina* spp. on off-mound core M125-50-3 with red horizontal shadings illustrating the $\delta^{18}O$ level during different isotope stages as used in panel (C); (H) the LR04 benthic stack (Lisiecki and Raymo, 2005) as an approximation for eustatic sea-level changes; Marine Isotope Stages (MIS) are
310 indicated by pink and blue bars signifying relatively warm and cold periods, respectively.

5. Results and Discussion

https://doi.org/10.5194/bg-2020-206
Preprint. Discussion started: 30 June 2020

In the following we discuss if and how changes in environmental parameters might have enhanced or prohibited CWC growth at Bowie Mound, focusing on the role of intermediate water-mass variability and varying terrigenous sediment supply.

5.1 Drivers and inhibitors of CWC growth at Bowie Mound

5.1.1 Intermediate water mass properties and hydraulic dynamics

Intermediate water mass properties might have played a crucial role for the development of Bowie Mound. First, Bowie Mound lies within the nutrient-rich AAIW, which might have boosted CWC growth at the East Brazilian slope. Second, nutrients and POC typically concentrate within nepheloid layers at water mass boundaries and provide a prolific food source for CWCs (Mienis et al., 2007; Dullo et al., 2008; Raddatz et al., 2014; Rüggeberg et al., 2016; Magill et al., 2018). In the case of Bowie Mound it might thus be suspected that enhanced production (Pahnke and Zahn, 2005; Pahnke et al., 2008) and/or nutrient-enrichment (i.e. increasing phosphate and nitrate concentration) of the AAIW (Poggemann et al., 2017) during phases of weak Atlantic Meridional Overturning Circulation (AMOC) could have triggered its episodic formation phases. A more prominent AAIW might have further strengthened internal waves hitting the slope at the AAIW/SACW boundary in the Campos Basin (Viana et al., 1998; Viana, 2001) and thus fueled the nepheloid layer by enhanced resuspension.

Here, we use the benthic $\delta^{13}C$ obtained on M125-34-2 as an indicator of the relative contribution of nutrient-rich (hence, ^{13}C depleted) southern-sourced intermediate water masses (Kroopnick, 1985; Curry and Oppo, 2005). As we had to use different species (shallow infaunal *Uvigerina* spp. and epibenthic *C. wuellerstorfi*) we combined both records. To adjust for intra-species offsets, we followed the approach of Kaboth et al. (2017) and normalized the $\delta^{13}C$ values of each species to the respective mean and standard deviation. The resultant normalized data, although exhibiting a considerable scatter, do not provide compelling evidence for distinctly depleted values during phases of CWC growth compared to CWC-barren intervals (Fig. 4). Albeit the $\delta^{13}C$ of *Uvigerina* spp. might be influenced by isotopic variations of dissolved inorganic carbon of pore-water (Zahn et al., 1986), we nevertheless consider it as appropriate to reconstruct profound changes in the bottom-water signature. Even when only considering the $\delta^{13}C$ values obtained on epibenthic *C. wuellerstorfi* no systematic difference between CWC-bearing and CWC-barren intervals becomes apparent. The continuous, monospecific *Uvigerina* spp. $\delta^{13}C$ record obtained on off-mound core M125-50-3 also lacks negative excursions during times of CWC growth at Bowie Mound (Fig. 5C). Hence, it appears that changes in the nutrient content of the AAIW as observed during the last deglaciation (Poggemann et al., 2017) did not significantly affect CWC growth.

https://doi.org/10.5194/bg-2020-206
Preprint. Discussion started: 30 June 2020

345

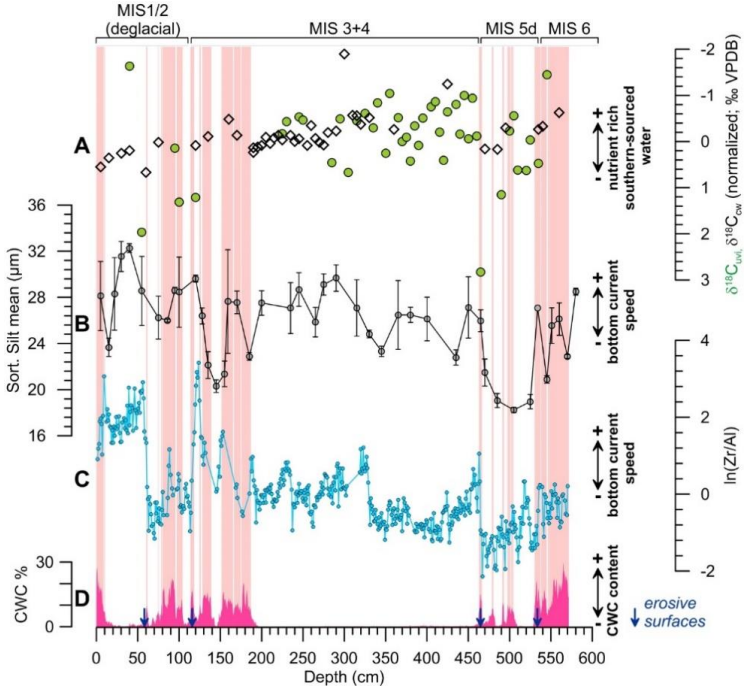

Fig. 4 Proxies of intermediate water mass variability *vs*. phases of mound formation obtained on Core M125-34-2. (A) normalized $\delta^{13}C$ of *Uvigerina* spp. (green dots) and *P. wuellerstorfi* (white diamonds) as a proxy for bottom water
350 mass origin and nutrient level, (B) mean sortable silt ($\overline{SS}$) reflecting bottom current speed, (C) XRF-derived sedimentary ln(Zr/Al) ratio depends on bottom current speed (Bahr et al., 2014) and advection of fine-grained material from the nepheloid layer, and (D) CWC abundances based on CT-scanning. Light red shadings denote intervals with coral contents >7 % used for discriminant analysis; blue arrows indicate erosive unconformities.

https://doi.org/10.5194/bg-2020-206
Preprint. Discussion started: 30 June 2020

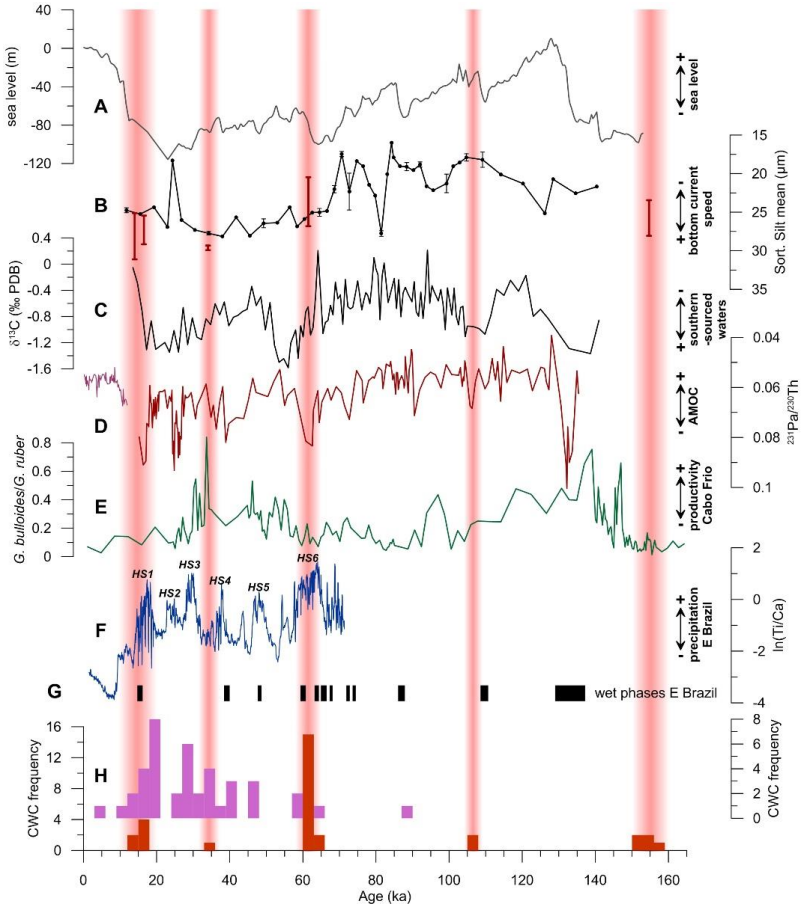

Fig. 5 Frequency of CWC occurrences in the time domain at Bowie Mound core M125-34-2 and adjacent cores from SE Brazilian Margin in the paleoclimatic context. (A) global sea level (Grant et al., 2012); (B) mean sortable silt in off-mound core M125-50-3, range of sortable silt values of CWC-bearing intervals in core M125-34-2 are indicated by red error bars; (C) benthic $\delta^{13}C$ of *Uvigerina* spp. in off-mound core M125-50-3 reflecting the portion of nutrient-rich southern-sourced waters (AAIW) at the SE Brazilian Margin; (D) variability of deep oceanic overturning circulation (dark red line: Böhm et al., 2015; purple: Lippold et al., 2019); (E) upwelling intensity at Cabo Frio reflected by the ratio between upwelling-related planktonic foraminifer *Globigerinoides bulloides* and oligotrophic *Globigerinoides ruber*; (F) Ti/Ca ratio reflecting terrigenous input to the E Brazilian margin off the Sao Francisco River (core M125-95-3; Campos et al., 2019); (G) growth periods of travertine and speleothems in E Brazil during anomalous wet periods, indicated by black bars (Wang et al., 2004); (H) frequency of CWC dates per 3 kyrs bins at Bowie Mound (core M125-34-2; red bars) and in cores at the SE Brazilian Margin (violet) (Mangini et al., 2010; Ruckelshausen, 2013) (Fig. 1). Red bars indicate periods of enhanced CWC growth at Bowie Mound.

While nutrient delivery by the AAIW seemed to had an insignificant effect on CWC growth at Bowie Mound, changes in the hydrodynamics regime altering the depth and strength of the nepheloid layer might have influenced mound

https://doi.org/10.5194/bg-2020-206
Preprint. Discussion started: 30 June 2020

formation. Hydrodynamic conditions at core M125-34-2 can be reconstructed by using the variation in $\overline{SS}$, a well-established proxy for bottom current speed reflected by the mean grain size of the 10-63 µm fraction (McCave et al., 1995), and the sedimentary Zr/Al ratio (Fig. 4). The latter proxy follows the rationale that heavy minerals accumulate relative to aluminosilicates during high bottom current flow speed (e.g., Turnewitsch et al., 2004; Bahr et al., 2014; Miramontes et al., 2019). The significant correlation ($r=+0.49$; $p<0.05$) of both proxies may therefore predominantly reflect the hydraulic regime at Bowie Mound, despite certain intervals where both parameters deviate (e.g. between 60–115 cm with high $\overline{SS}$ and low Zr/Al values), which might be due to small-scale hydraulic effects created by the CWC branches themselves (Mienis et al., 2019). Based on both hydrodynamic proxies, CWC at Bowie Mound tend to accumulate in intervals with elevated flow speed. Phases of low flow speed are accompanied by low CWC abundances (e.g., between 140–150 cm and 465–550 cm), in line with the notion that active bottom currents play a significant role in distributing nutrients and food towards CWC colonies (e.g., Thiem et al., 2006; Dorschel et al., 2007; Davies et al., 2009; Raddatz et al., 2011). High current speeds will also increase sediment and POC supply, thereby providing food and at the same time increase accumulation rates due to the baffling capacity of CWC. Our data, however, suggest that a relatively high flow speed does not necessarily led to CWC growth as demonstrated by the extended CWC-free section between 200–460 cm, where Zr/Al and $\overline{SS}$ fluctuates on a relatively high level as well as between 15–60 cm where no CWC are preserved despite high TOC accumulation. Hence, the absence of CWC-bearing intervals despite persistently high bottom current speeds during most of the glacial intervals MIS 3 and 4 indicate that additional environmental drivers other than intermediate water mass variability must play an active role for CWC growth at the Brazilian Margin.

5.1.2 Terrestrial and marine organic matter supply

The prerequisite for enhanced CWC growth is sufficient food supply to Bowie Mound. To assess the potential impact of enhanced POC and/or DOC supply as an incentive for enhanced CWC growth we compared TOC measurements to CWC abundances (Fig. 6). It appears that CWC abundances are highest in intervals with elevated OM presence, which stresses its importance as a prerequisite for mound aggregation. While statistically significant, the down-core pattern of CWC abundances and TOC ($r = 0.55$; $p < 0.05$) also indicates that this correlation is not straight forward; an example is the interval between 15–60 cm with high TOC contents that is barren of corals (Fig. 6). As argued also in the previous section, there have been multiple factors necessary to stimulate coral growth at Bowie Mound.

https://doi.org/10.5194/bg-2020-206
Preprint. Discussion started: 30 June 2020

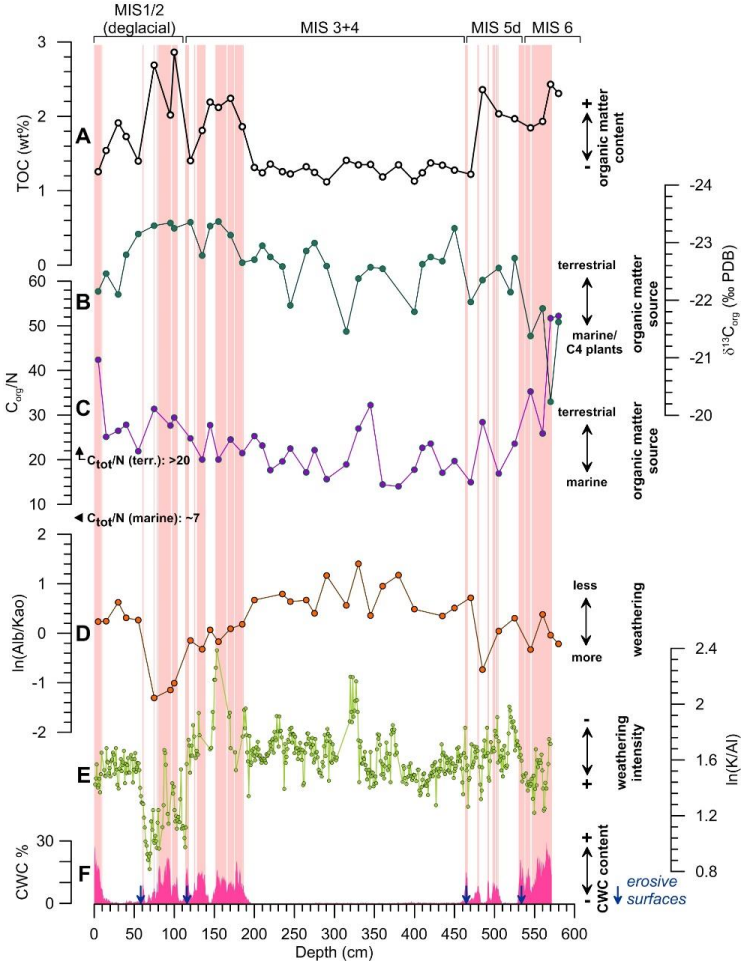

Fig. 6 Organic-matter accumulation and origin at Bowie Mound core M125-34-2 in context with continental hydroclimate and CWC occurrences. (A) Total organic carbon (TOC, white dots) reflecting organic-matter accumulation; (B) and (C) $\delta^{13}C$ and C_{org}/N_{tot} ratio of organic matter as measures for terrestrial *vs.* marine organic matter input, respectively. Marine and terrestrial endmembers are indicated (Holtvoeth et al., 2003); (D) and (E) XRD-derived ln(Albite/Kaolinite) and XRF-derived ln(K/Al) ratios, respectively, as indicators of the weathering intensity in the hinterland, reflecting the strength of the continental hydrological cycle; and (F) CWC abundances based on CT-scanning. Light red shadings denote intervals with coral contents >7 % used for discriminant analysis; blue arrows indicate erosive unconformities.

To investigate the origin of the organic matter within the sediment matrix we analyzed its C_{org}/N_{total} ratio and stable carbon isotopic composition ($\delta^{13}C_{org}$). Marine organic matter has lower C_{org}/N_{total} ratios (~6.6) compared to terrestrial organic matter (>20) (Holtvoeth et al., 2003). Organic matter in core M125-34-2 exhibits C_{org}/N_{total} ratios of 14 to 52 (Fig. 6), indicating that land-derived material has been an significant source of organic matter throughout the record.

https://doi.org/10.5194/bg-2020-206
Preprint. Discussion started: 30 June 2020

Intervals with CWC abundances are thereby characterized by elevated C_{org}/N_{total} ratios, namely at the top and at the base of the core with ratios >40, pointing at an overwhelming contribution of terrigenous matter. Notably, organic matter derived from upwelling on the shelf off Cabo Frio apparently plays a subordinate role as this predominantly marine organic material has low C_{org}/N_{total} ratios typically below 6.5 (Albuquerque et al., 2014) in line with the upwelling center being confined to the shelf without reaching northward to the slope where Bowie Mound is situated (Albuquerque et al., 2014, 2016). A significant terrigenous admixture of terrestrial organic matter is also indicated by the relatively low $\delta^{13}C_{org}$ (-23.2 to -20.2 ‰) as terrigenous organic material has a more depleted signature (-27 ‰) compared to typical marine $\delta^{13}C_{org}$ values (-19 ‰) (Holtvoeth et al., 2003). In this regard, low $\delta^{13}C_{org}$ values during CWC-bearing intervals in the upper 50 cm and below 549.5 cm might be interpreted as enhanced marine productivity, which is in contradiction to parallel C_{org}/N_{total} ratios as high as 52. This conflicting evidence might be resolved by interpreting the high $\delta^{13}C_{org}$ values as representing enhanced input of POC from C4 plants (typically grasses), which are characterized by an endmember of ca. -12 ‰ (Holtvoeth et al., 2003). Palynological evidence in fact point to the establishment of grassland biomes in the catchment of the Paraiba do Sul during the last glacial caused by generally drier conditions (Behling et al., 2002). This is in accord with the presumed deposition of the intervals 0–50 cm and 549.5–568 cm during the last deglaciation and MIS 6, respectively (Fig. 5).

5.1.3 Influence of the continental hydrological cycle

A major source of terrigenous material and thus a potent organic-matter source for the Brazilian Margin are rivers draining the densely vegetated hinterland, especially the Paraiba do Sul (Fig. 1). To investigate if enhanced riverine input due to more humid conditions in the hinterland contributed to enhanced terrestrial organic-matter supply to Bowie Mound, we studied the mineralogical and geochemical composition of the terrigenous fraction of the sediment. Changes in the water availability in the hinterland should impact the degree of weathering and thus leave an imprint in the mineralogical composition of the terrigenous sediments. The composition of the non-carbonaceous mineral phases is typical for soils that underwent different degrees of chemical weathering, comprising intermediate weathering products such as hydrobiotite (11.5 %, up to 24 %) (Coleman et al., 1963; Wilson, 1970; Meunier and Velde, 1979), as well as typical constituents of soils that have been deeply weathered under tropical humid conditions such as kaolinite (7.9 % up to 15.3 %), gibbsite (on average 21.7 %) and Ca, K, Al-rich Zeolite (6.7 %) (e.g. Weaver, 1975; Hughes, 1980; Ibrahim and Hall, 1996; Furian et al., 2002) (cf. Appendix Table A). When comparing minerals typical for residual soils such as kaolinite, gibbsite, and zeolite with feldspar and mica, both groups are anti-correlated (Table XRD) and exhibit distinct fluctuations throughout the core (cf. the albite *vs*. kaolinite ratio is depicted in Fig. 6). Relatively high abundances of weathering residuals like kaolinite are particularly present in the CWC-bearing interval between ca. 60 to 200 cm and (to a lesser extend) below 560 cm. This XRD-based data is also partly supported by the high-resolution K/Al record obtained via XRF scanning, which is particularly low during the interval 60–120 cm and below 530 cm (Fig. 6). Low K/Al ratios are in line with high kaolinite contents reflecting periods of strong K-removal from soils due to chemical weathering under humid conditions in the hinterland. As the C_{org}/N_{total} ratio is also elevated during periods of low K/Al ratios and high kaolinite contents (Fig. 6), it can be inferred that high precipitation in the hinterland fostered chemical weathering in combination with elevating terrigenous organic matter transport to the continental slope. Stronger chemical weathering would have also enhanced the input of Fe to the continental slope

https://doi.org/10.5194/bg-2020-206
Preprint. Discussion started: 30 June 2020

(Govin et al., 2012) leading to fertilization of the surface waters, which might have additionally invigorated surface productivity and thus food for CWC at Bowie Mound.

Table XRD: Correlation between terrigenous mineral phases in core M125-34-2. Positive correlations are marked in red (for r>0.4), negative correlations (for r<0.4) in blue.

	Quartz	Gibbsite	Kaolinite	Muscovite	Hydrobiotite	Microcline	Zeolite
Quartz							
Gibbsite	-0.07						
Kaolinite	-0.52	-0.09					
Muscovite	0.35	0.45	-0.31				
Hydrobiotite	-0.34	-0.62	0.55	-0.69			
Microcline	0.49	-0.26	-0.43	-0.15	-0.02		
Zeolite	-0.16	0.68	0.00	0.62	-0.43	-0.51	
Albite	0.65	-0.07	-0.76	0.47	-0.44	0.35	-0.07

To objectively evaluate the relative importance of terrestrial matter supply over changes in the hydraulic conditions potentially influencing CWC proliferation at Bowie Mound we performed a discriminant analysis over n=34 samples using (i) ln(Alb/Kao) as a weathering proxy, (ii) $\overline{SS}$ for bottom current speed, (iii) $\delta^{13}C_{org}$, and (iv) C_{org}/N_{total} for organic matter provenance as predictors for the occurrences of CWC abundances above 7 % (reflecting representative CWC accumulations). Note that the $\delta^{13}C$ of benthic foraminifera had not been included due to the high scatter of the data. The restriction on those four parameters was also done to avoid unreliable results by over-prediction. The outcome of the discriminant analysis yields a correct classification of 76 % with highest skills in ln(Alb/Kao) (loading of -0.68) and C_{org}/N_{total} (+0.58), while loadings for $\overline{SS}$ (+0.06) and $\delta^{13}C$ org (0.00) are insignificant (see Appendix Table B for details). This is in line with peak CWC abundances synchronous to phases of a strong hydrological cycle as reflected by intensified chemical weathering (i.e. low ln(Alb/Kao) ratios) which triggered a strong input of terrigenous organic matter with a high C_{org}/N_{total} ratio to Bowie Mound directly or indirectly fueling CWC proliferation.

5.2 CWC at Bowie Mound in the paleoclimatological context

As discussed above, phases of enhanced CWC proliferation at Bowie Mound occurred parallel to increased POC and/or DOC input from land due to enhanced run-off. Within age model uncertainties, the most distinct CWC proliferation phases in fact took place during phases of anomalously humid conditions in E Brazil associated with Heinrich Stadials (HS) 1, 4, and 6 (Fig. 5F, G). The prominent growth phase during HS is well in agreement with published CWC occurrences during the same time frame along the SE Brazilian Margin (Mangini et al., 2010; Ruckelshausen, 2013) (Figs. 1, 5G), corroborating that our results are representative for a larger geographic area. The slow overturning circulation during HS indicated by high $^{231}Pa/^{230}Th$ ratios (McManus et al., 2004; Böhm et al., 2015) (Fig. 5 D) caused enhanced precipitation over south-eastern and eastern Brazil (Waelbroeck et al., 2018) as it led to heat accumulation in the southern hemisphere and thereby strengthening of the South Atlantic Convergence Zone (Stríkis et al., 2015) (Fig 1). Humid phases during HS in otherwise dry eastern Brazil are documented by growth phases of speleothems and travertines (Fig. 5G), increased terrigenous matter input (core M125-95-3; Fig. 5F) (Campos et al., 2019), and a

https://doi.org/10.5194/bg-2020-206
Preprint. Discussion started: 30 June 2020

slight expansion of forest cover (Gu et al., 2018). It might thus be argued that the riverine suspension load from rivers in eastern Brazil was advected southward by the BC and added to the enhanced river load from rivers adjacent to Bowie Mound (mostly the Paraiba do Sul). Due to their baffling capacity, the additional sedimentary input would have aided mound formation. This nutrient and organic-rich suspension potentially also enhanced marine surface productivity and thus directly and/or indirectly boosted food supply to the CWC. As freshwater admixture to the SMW and SACW might have caused a more pronounced water column stratification and hence increased density contrast to the AAIW, the concentration of sediment and food particles at the nepheloid layer might have been more pronounced as well.

Notably, HS occurred during phases of intermediate and low sea level, which facilitated the bypass of sediment across the shelf and thus allowed for an efficient supply of terrestrial OM to Bowie Mound (Fig. 5A). As discussed in Raddatz et al. (2020), a low sea level might have also forced water-mass boundaries to migrate downslope during glacials, when sea level was considerably lower by up to 120 m than today (Waelbroeck et al., 2002; Rohling et al., 2014). Such a displacement of water-mass boundaries would have moved the SACW/AAIW interface and the corresponding nepheloid layer from its present position at ~500 m closer to the depth of Bowie Mound (~860 m) aiding the concentration and dispersal of food along the slope towards the CWC colonies. This suspected influence of sea level on the bottom-current dynamics in the depth of Bowie Mound is in fact evident from a sortable silt record obtained on off-mound site M125-50-3, which shows high (low) current speeds during low (high) sea level (Fig. 5B).

Hence, it might be argued that for CWC to flourish at Bowie Mound a dynamic hydraulic regime was required with a pronounced nepheloid layer such as prevailing throughout glacial periods (Mienis et al., 2007). The development of wide-spread glacial unconformities and extensive drift bodies at the south-east Brazilian margin (Viana et al., 1998; Viana, 2001) are evidence for such intense bottom-current activity. This is notably different from the slope south of the Abrolhos Bank where reference core M125-50-3 is situated. Here, contouritic sediments and distinct hiatuses are largely absent in water depths affected by the AAIW and SACW testify for less dynamic hydrological conditions (Bahr et al., 2016), potentially explaining the lack of CWC mounds at this location. At the same time, $\overline{SS}$ and Zr/Al data from neither Bowie Mound core M125-34-2 (Fig. 4B) nor off-mound site M125-50-3 (Fig. 5B) indicate that bottom-current speed has been anomalously high during HS relative to the glacial background level. Hence, the distinct, pulse-like CWC growth phases at Bowie Mound could have been ultimately initiated by enhanced nutrient and organic matter supply from land as evidenced by the high C_{org}/N ratio of the organic matter. Due to ensuing fertilization of the surface waters, marine primary productivity might also have been enhanced and contributed to higher export production, additionally fueling CWC growth. As discussed before, marine productivity derived from upwelling on the shelf of Cabo Frio was apparently of minor importance. Based on planktic foraminiferal assemblages (Lessa et al., 2019), enhanced upwelling occurred between HS 3 and 4, at around 35 kys, when a small peak of CWC occurs (Fig. 5G). However, at all other instances of CWC occurrences, upwelling at Cabo Frio appears rather low and there is no evidence that it reached as far north as Bowie Mound (Albuquerque et al., 2014, 2016).

We hence infer that CWC proliferation at Bowie Mound occurred simultaneously with an enhanced delivery of terrestrial organic matter towards the continental slope under glacial boundary conditions of low sea level and enhanced hydrodynamic activity along the slope. As this temporal coincidence could point at the direct utilization of terrestrial

https://doi.org/10.5194/bg-2020-206
Preprint. Discussion started: 30 June 2020

organic matter by the corals, it clearly stresses the necessity for future in-depth studies of the food preferences of *S. variabilis*.

520

Conclusions

Here we present a comprehensive multi-proxy study of a cold-water coral (CWC)-bearing core retrieved off SE Brazil with the aim to assess the relative importance of different environmental factors that supported and/or prohibited CWC proliferation and coral mound formation. We find that intervals of high CWC abundances are primarily related to
525 millennial-scale high latitude cold events (Heinrich Stadials) that were characterized by major reconfigurations of the deep-ocean circulation and an enhanced continental hydrological cycle in eastern Brazil. The dominance of terrigenous- over marine-derived organic matter during phases of fast CWC proliferation indicate that strong run-off enhanced the input of nutrients and food to the coral mounds on the continental slope. Intensified hydrodynamic conditions on intermediate water level during sea level lowstands thereby provided the necessary background
530 conditions for an efficient dispersal of nutrient and food supply towards the upper and mid slope. This study thus presents a prime example of the high sensitivity of deep marine ecosystems to changes in the environmental conditions and points at a hitherto unrecognized intimate coupling between continental hydroclimate and ecological changes in the deep ocean.

535

https://doi.org/10.5194/bg-2020-206
Preprint. Discussion started: 30 June 2020

Biogeosciences Discussions

Appendices

Appendix Table A: Major non-carbonaceous mineral phases in core M125-34-2 derived from Rietveld analyses of X-ray diffractometry.

Depth (cm)	Quartz	Gibbsite	Kaolinite	Muscovite	Hydrobiotite	Microcline	Zeolite	Albite
	(%)	(%)	(%)	(%)	(%)	(%)	(%)	(%)
5	8.5	20.2	5.7	5.6	7.8	7.0	6.7	7.2
15	8.0	19.1	7.8	5.5	16.1	4.6	6.7	10.0
30	6.9	18.7	6.5	2.1	10.1	6.3	4.2	12.1
40	7.6	20.3	7.7	3.4	17.1	9.3	3.8	10.5
55	10.4	18.4	8.7	4.0	14.1	3.7	5.0	11.3
75	4.6	20.0	15.3	4.8	20.2	2.1	6.5	4.2
95	4.3	17.6	12.0	4.4	21.7	4.8	5.9	3.8
100	4.8	16.4	12.6	5.6	24.0	3.2	6.2	4.6
120	9.7	15.5	10.3	4.4	18.2	6.2	4.7	8.9
135	8.3	24.5	9.9	9.4	12.9	4.3	6.7	7.2
145	7.1	24.1	9.0	5.1	17.4	3.3	7.1	9.6
155	7.8	25.9	10.2	11.5	7.8	4.6	7.9	8.6
170	7.6	22.3	9.0	6.1	17.6	4.0	7.1	9.8
185	9.2	25.1	7.4	11.5	6.0	6.2	7.4	8.9
200	10.2	21.3	6.2	6.2	12.5	7.9	6.6	12.2
235	9.2	20.6	5.4	13.3	10.7	3.6	7.4	12.0
245	9.5	22.6	6.5	13.2	5.7	5.8	6.8	12.4
265	8.1	22.8	6.5	9.9	9.8	6.4	7.4	12.7
275	9.2	23.5	7.5	12.9	6.9	5.4	7.0	11.3
290	9.6	21.6	4.0	10.7	9.7	6.9	6.3	13.0
315	10.4	21.9	6.3	12.8	7.1	5.0	6.7	11.1
330	9.3	19.8	4.0	11.4	8.7	5.1	6.4	16.3
345	7.7	19.7	8.3	11.9	10.2	4.9	7.1	11.9
360	6.9	19.4	5.5	9.0	10.0	5.8	6.3	14.3
380	8.3	23.1	4.5	13.7	5.2	3.2	7.2	14.5
400	7.0	21.2	6.2	7.6	12.9	6.8	6.5	10.1
435	7.9	23.1	8.3	12.6	6.2	3.1	6.8	11.8
450	7.8	23.1	7.0	12.0	7.4	3.8	7.4	11.7
470	8.3	18.6	6.4	11.8	14.6	4.6	7.5	13.2
485	6.3	27.4	12.2	12.3	5.5	2.8	8.5	5.8
505	5.5	23.7	9.5	12.5	6.2	2.8	7.7	9.9
525	5.7	24.6	7.4	10.2	11.2	3.6	8.0	10.1
545	4.4	23.1	8.4	4.4	10.3	3.0	7.4	6.0
560	6.5	26.3	5.3	6.8	8.1	3.8	7.1	7.8

https://doi.org/10.5194/bg-2020-206
Preprint. Discussion started: 30 June 2020

Biogeosciences Discussions Open Access EGU

570	5.8	22.0	7.3	6.0	10.5	3.5	6.4	7.0
580	5.3	23.0	8.1	5.8	12.9	2.8	7.3	6.5

APPENDIX Table B. Result of discriminant analysis performed on detrended and normalized proxies obtained on core M125-34-2. Samples were divided into classes with CWC contents >7% (labelled "1") and <7% ("0"). Classes derived from discriminant analysis are displayed in the last column, with wrong calls marked in red.

depth (cm)	ln(Alb/Kao)	$\overline{SS}$ (µm)	$\delta^{13}C_{org}$ (‰ PDB)	C_{org}/N	CWC > 7%	inferred class
5	0.01	0.71	0.58	2.03	1	1
15	0.03	-0.61	0.11	0.04	0	0
30	0.64	1.73	0.67	0.20	0	0
40	0.13	1.94	-0.39	0.35	0	0
55	0.06	0.84	-0.95	-0.33	0	0
75	-2.49	0.15	-1.17	0.77	1	1
95	-2.23	0.86	-1.24	0.33	1	1
100	-2.01	0.81	-1.10	0.54	1	1
120	-0.61	1.16	-1.25	0.00	0	1
135	-0.89	-1.07	-0.37	-0.55	1	0
145	-0.26	-1.61	-1.16	0.35	0	0
155	-0.65	-1.30	-1.28	-0.54	1	0
170	-0.22	0.54	-0.91	-0.03	1	0
185	-0.08	-0.85	-0.18	-0.38	1	0
200	0.72	0.53	-0.26	0.06	0	0
235	0.92	0.40	-0.08	-0.60	0	0
245	0.67	0.88	0.95	-0.26	0	0
265	0.72	0.04	-0.49	-0.88	0	0
275	0.29	1.00	-0.71	-0.30	0	0
290	1.53	1.17	-0.09	-1.06	0	0
315	0.55	0.40	1.65	-0.68	0	0
330	1.91	-0.27	0.24	0.25	0	0
345	0.21	-0.72	-0.06	0.86	0	0
400	0.42	0.12	1.12	-0.80	0	0
435	0.20	-0.87	-0.22	-0.88	0	0
450	0.46	0.41	-1.10	-0.59	0	0
470	0.80	-1.26	0.86	-1.13	0	0
485	-1.56	-1.98	0.28	0.42	0	1
505	-0.30	-2.22	-0.04	-0.91	0	0
525	0.13	-2.01	-0.30	-0.13	0	0
545	-0.90	-1.44	1.77	1.21	0	1
560	0.24	0.11	1.03	0.13	1	0
570	-0.43	-0.85	3.52	3.12	1	1
580	-0.72	0.82	1.40	3.17	1	1

https://doi.org/10.5194/bg-2020-206
Preprint. Discussion started: 30 June 2020


Biogeosciences
Discussions
Open Access
EGU

https://doi.org/10.5194/bg-2020-206
Preprint. Discussion started: 30 June 2020

550

Appendix Figure A: CT image (left) and photography (right) of segment 0-83 cm of core M125-34-2. Erosional contacts are marked by thick black lines, position of Th/U datings with calibrated ages are indicated by magenta dots.

https://doi.org/10.5194/bg-2020-206
Preprint. Discussion started: 30 June 2020

Biogeosciences
Discussions
Open Access
EGU

Appendix Figure B: CT image (left) and photography (right) of segment 83-183 cm of core M125-34-2. Erosional contacts are marked by thick black lines, position of Th/U datings with calibrated ages are indicated by magenta dots.

https://doi.org/10.5194/bg-2020-206
Preprint. Discussion started: 30 June 2020

Biogeosciences
Discussions
Open Access
EGU

Appendix Figure C: CT image (left) and photography (right) of segment 183-283 cm of core M125-34-2. Position of Th/U dating with calibrated age is indicated by a magenta dot.

https://doi.org/10.5194/bg-2020-206
Preprint. Discussion started: 30 June 2020

560

Appendix Figure D: CT image (left) and photography (right) of segment 283-383 cm of core M125-34-2.

https://doi.org/10.5194/bg-2020-206
Preprint. Discussion started: 30 June 2020

Biogeosciences
Discussions
Open Access
EGU

Appendix Figure E: CT image (left) and photography (right) of segment 383-483 cm of core M125-34-2. Erosional contacts are marked by thick black lines, position of Th/U dating with calibrated age is indicated by a magenta dot.

https://doi.org/10.5194/bg-2020-206
Preprint. Discussion started: 30 June 2020

Biogeosciences
Discussions
Open Access
EGU

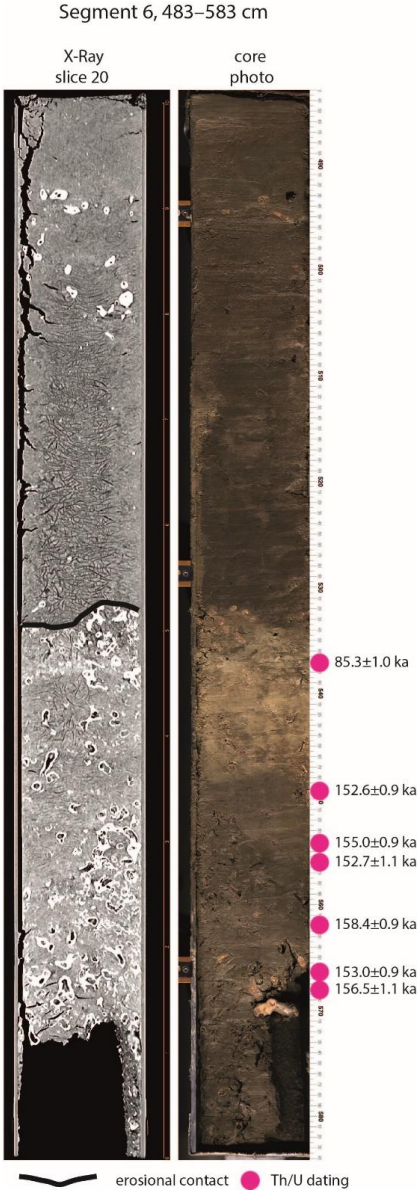

Appendix Figure F: CT image (left) and photography (right) of segment 383-483 cm of core M125-34-2. Erosional contacts are marked by thick black lines, positions of Th/U datings with calibrated age are indicated by magenta dots**.**

570 **Data availability**

All data presented in this study will be made available in the Pangaea data base (www.pangaea.de).

Author contribution

https://doi.org/10.5194/bg-2020-206
Preprint. Discussion started: 30 June 2020

AB and JR designed the study. AB, MD, JT, GA, DN, and JR were involved in sampling and data generation. All authors contributed to data interpretation and manuscript writing.

Competing Interests

The authors declare that they have no conflict of interest.

Acknowledgements:

We thank Captain and crew of R/W Meteor for their support during Expedition M125. We further kindly acknowledge I. Glass (X-Ray diffractometry), A. Koutsodendris (XRF-scanning), D. Bergmann-Dörr (carbon and nitrogen analysis), S. Brzelinski, C. Catunda, S. Fessler, J. Fiebig, S. Hofmann, B. Knape, (stable oxygen and carbon isotope analysis), N. Gehre (sample preparation and foraminiferal selection), L. Frede (sortable silt analysis), for support during sample preparation and analyses. The authors are grateful to W. Stiller and S. Skornitzke from the Heidelberg University Hospital for performing the CT scanning. AB was funded by the Deutsche Forschungsgemeinschaft (DFG project HO5927/1-1). JT received funds from the MARUM Cluster of Excellence 'The Ocean Floor – Earth's Uncharted Interface' (Germany´s Excellence Strategy – EXC-2077 – 390741603 of the Deutsche Forschungsgemeinschaft DFG).

References

Addamo, A. M., Vertino, A., Stolarski, J., García-Jiménez, R., Taviani, M., and Machordom, A.: Merging scleractinian genera: the overwhelming genetic similarity between solitary *Desmophyllum* and colonial *Lophelia*, BMC evolutionary biology, 16, 108, 2016.

Aguiar, A. L., Cirano, M., Pereira, J., and Marta-Almeida, M.: Upwelling processes along a western boundary current in the Abrolhos–Campos region of Brazil, Continental Shelf Research, 85, 42-59, https://doi.org/10.1016/j.csr.2014.04.013, 2014.

Albuquerque, A. L., Meyers, P., Belem, A. L., Turcq, B., Siffedine, A., Mendoza, U., and Capilla, R.: Mineral and elemental indicators of post-glacial changes in sediment delivery and deposition under a western boundary upwelling system (Cabo Frio, southeastern Brazil), Palaeogeography, Palaeoclimatology, Palaeoecology, 445, 72-82, http://dx.doi.org/10.1016/j.palaeo.2016.01.006, 2016.

Albuquerque, A. L. S., Belem, A. L., Zuluaga, F. J., Cordeiro, L. G., Mendoza, U., Knoppers, B. A., Gurgel, M. H., Meyers, P. A., and Capilla, R.: Particle fluxes and bulk geochemical characterization of the Cabo Frio upwelling system in Southeastern Brazil: Sediment trap experiments between Spring 2010 and Summer 2012, Anais da Academia Brasileira de Ciências, 86, 601-620, 2014.

Bahr, A., Jiménez-Espejo, F. J., Kolasinac, N., Grunert, P., Hernández-Molina, F. J., Röhl, U., Voelker, A. H., Escutia, C., Stow, D. A., and Hodell, D.: Deciphering bottom current velocity and paleoclimate signals from contourite deposits in the Gulf of Cádiz during the last 140 kyr: An inorganic geochemical approach, Geochemistry, Geophysics, Geosystems, 15, 3145-3160, 10.1002/ggge.20106, 2014.

Bahr, A., Spadano Albuquerque, A., Ardenghi, N., Batenburg, S., Bayer, M., Catunda, M., Conforti, A., Dias, B., Dias Ramos, R., and Egger, L.: South American Hydrological Balance and Paleoceanography during the Late Pleistocene and Holocene (SAMBA)–Cruise No. M125, March 21–April 15, 2016-Rio de Janeiro (Brazil)–Fortaleza (Brazil), 2016.

Behling, H., Arz, H. W., Pätzold, J., and Wefer, G.: Late Quaternary vegetational and climate dynamics in southeastern Brazil, inferences from marine cores GeoB 3229-2 and GeoB 3202-1, Palaeogeography, Palaeoclimatology, Palaeoecology, 179, 227-243, 2002.

Bianchi, G. G., Vautravers, M. J., and Shackleton, N. J.: Deep flow variability under apparently stable North Atlantic Deep Water production during the last interglacial of the subtropical NW Atlantic, Paleoceanography, 16, 306-316, 2001.

https://doi.org/10.5194/bg-2020-206
Preprint. Discussion started: 30 June 2020

Böhm, E., Lippold, J., Gutjahr, M., Frank, M., Blaser, P., Antz, B., Fohlmeister, J., Frank, N., Andersen, M. B., and Deininger, M.: Strong and deep Atlantic meridional overturning circulation during the last glacial cycle, Nature, 517, 73-76, 10.1038/nature14059, 2015.

Bostock, H. C., Tracey, D. M., Currie, K. I., Dunbar, G. B., Handler, M. R., Fletcher, S. E. M., Smith, A. M., and Williams, M. J.: The carbonate mineralogy and distribution of habitat-forming deep-sea corals in the southwest pacific region, Deep Sea Research Part I: Oceanographic Research Papers, 100, 88-104, 2015.

Büscher, J. V., Form, A. U., and Riebesell, U.: Interactive effects of ocean acidification and warming on growth, fitness and survival of the cold-water coral *Lophelia pertusa* under different food availabilities, Frontiers in Marine Science, 4, 101, 2017.

Campos, M. C., Chiessi, C. M., Prange, M., Mulitza, S., Kuhnert, H., Paul, A., Venancio, I. M., Albuquerque, A. L. S., Cruz, F. W., and Bahr, A.: A new mechanism for millennial scale positive precipitation anomalies over tropical South America, Quaternary Science Reviews, 225, 105990, https://doi.org/10.1016/j.quascirev.2019.105990, 2019.

Carvalho, C., Salomão, M., Molisani, M., Rezende, C., and Lacerda, L.: Contribution of a medium-sized tropical river to the particulate heavy-metal load for the South Atlantic Ocean, Science of the Total Environment, 284, 85-93, 2002.

Carvalho, L. M., Jones, C., and Liebmann, B.: The South Atlantic convergence zone: Intensity, form, persistence, and relationships with intraseasonal to interannual activity and extreme rainfall, Journal of Climate, 17, 88-108, 2004.

Castelao, R. M., and Barth, J. A.: The relative importance of wind strength and along-shelf bathymetric variations on the separation of a coastal upwelling jet, Journal of Physical Oceanography, 36, 412-425, 2006.

Castelao, R. M.: Sea surface temperature and wind stress curl variability near a cape, Journal of Physical Oceanography, 42, 2073-2087, 2012.

Cathalot, C., Van Oevelen, D., Cox, T. J., Kutti, T., Lavaleye, M., Duineveld, G., and Meysman, F. J.: Cold-water coral reefs and adjacent sponge grounds: Hotspots of benthic respiration and organic carbon cycling in the deep sea, Frontiers in Marine Science, 2, 37, 2015.

Coleman, N., LeRoux, F., and CADY, J. G.: Biotite-hydrobiotite-vermiculite in soils, Nature, 198, 409-410, 1963.

Curry, W. B., and Oppo, D. W.: Glacial water mass geometry and the distribution of $\delta^{13}C$ of ΣCO_2 in the western Atlantic Ocean, Paleoceanography, 20, PA1017, 2005.

Davies, A. J., Duineveld, G. C., Lavaleye, M. S., Bergman, M. J., van Haren, H., and Roberts, J. M.: Downwelling and deep-water bottom currents as food supply mechanisms to the cold-water coral *Lophelia pertusa* (Scleractinia) at the Mingulay Reef Complex, Limnology and Oceanography, 54, 620-629, 2009.

Dorschel, B., Hebbeln, D., Foubert, A., White, M., and Wheeler, A.: Hydrodynamics and cold-water coral facies distribution related to recent sedimentary processes at Galway Mound west of Ireland, Marine Geology, 244, 184-195, 2007.

Duineveld, G. C., Lavaleye, M. S., Bergman, M. J., De Stigter, H., and Mienis, F.: Trophic structure of a cold-water coral mound community (Rockall Bank, NE Atlantic) in relation to the near-bottom particle supply and current regime, Bulletin of Marine Science, 81, 449-467, 2007.

Dullo, W.-C., Flögel, S., and Rüggeberg, A.: Cold-water coral growth in relation to the hydrography of the Celtic and Nordic European continental margin, Marine Ecology Progress Series, 371, 165-176, 2008.

Fallon, S., Thresher, R., and Adkins, J.: Age and growth of the cold-water scleractinian *Solenosmilia variabilis* and its reef on SW Pacific seamounts, Coral Reefs, 33, 31-38, 2014.

Flögel, S., Dullo, W.-C., Pfannkuche, O., Kiriakoulakis, K., and Rüggeberg, A.: Geochemical and physical constraints for the occurrence of living cold-water corals, Deep Sea Research Part II: Topical Studies in Oceanography, 99, 19-26, 2014.

Form, A. U., and Riebesell, U.: Acclimation to ocean acidification during long-term CO_2 exposure in the cold-water coral *Lophelia pertusa*, Global Change Biology, 18, 843-853, 2012.

Frank, N., Freiwald, A., Correa, M. L., Wienberg, C., Eisele, M., Hebbeln, D., Van Rooij, D., Henriet, J.-P., Colin, C., and van Weering, T.: Northeastern Atlantic cold-water coral reefs and climate, Geology, 39, 743-746, 2011.

Frederiksen, R., Jensen, A., and Westerberg, H.: The distribution of the scleractinian coral *Lophelia pertusa* around the Faroe Islands and the relation to internal tidal mixing, Sarsia, 77, 157-171, 1992.

Furian, S., Barbiero, L., Boulet, R., Curmi, P., Grimaldi, M., and Grimaldi, C.: Distribution and dynamics of gibbsite and kaolinite in an oxisol of Serra do Mar, southeastern Brazil, Geoderma, 106, 83-100, 2002.

Gammon, M. J., Tracey, D. M., Marriott, P. M., Cummings, V. J., and Davy, S. K.: The physiological response of the deep-sea coral *Solenosmilia variabilis* to ocean acidification, PeerJ, 6, e5236, 2018.

Gori, A., Grover, R., Orejas, C., Sikorski, S., and Ferrier-Pagès, C.: Uptake of dissolved free amino acids by four cold-water coral species from the Mediterranean Sea, Deep Sea Research Part II: Topical Studies in Oceanography, 99, 42-50, 2014.

https://doi.org/10.5194/bg-2020-206
Preprint. Discussion started: 30 June 2020

Govin, A., Holzwarth, U., Heslop, D., Ford Keeling, L., Zabel, M., Mulitza, S., Collins, J. A., and Chiessi, C. M.: Distribution of major elements in Atlantic surface sediments (36°N–49°S): Imprint of terrigenous input and continental weathering, Geochemistry, Geophysics, Geosystems, 13, 2012.

Grant, K. M., Rohling, E. J., Bar-Matthews, M., Ayalon, A., Medina-Elizalde, M., Ramsey, C. B., Satow, C., and Roberts, A. P.: Rapid coupling between ice volume and polar temperature over the past 150,000 years, Nature, 491, 744-747, 10.1038/nature11593, 2012.

Gu, F., Chiessi, C. M., Zonneveld, K. A. F., and Behling, H.: Late Quaternary environmental dynamics inferred from marine sediment core GeoB6211-2 off southern Brazil, Palaeogeography, Palaeoclimatology, Palaeoecology, 496, 48-61, https://doi.org/10.1016/j.palaeo.2018.01.015, 2018.

Hammer, Ø., Harper, D. A. T., and Ryan, P. D.: PAST: Paleontological statistics software package for education and data analysis, Palaeontologica Electronica, 4, 9pp., 2001.

Hebbeln, D., Wienberg, C., Wintersteller, P., Freiwald, A., Becker, M., Beuck, L., Dullo, W.-C., Eberli, G. P., Glogowski, S., and Matos, L.: Environmental forcing of the Campeche cold-water coral province, southern Gulf of Mexico, Biogeosciences (BG), 11, 1799-1815, 2014.

Hebbeln, D., Portilho-Ramos, R. d. C., Wienberg, C., and Titschack, J.: The fate of cold-water corals in a changing world: a geological perspective, Frontiers in Marine Science, 2019.

Hennige, S., Wicks, L., Kamenos, N., Perna, G., Findlay, H., and Roberts, J.: Hidden impacts of ocean acidification to live and dead coral framework, Proceedings of the Royal Society B: Biological Sciences, 282, 20150990, 2015.

Hernández-Molina, F. J., Stow, D. A. V., Alvarez-Zarikian, C. A., Acton, G., Bahr, A., Balestra, B., Ducassou, E., Flood, R., Flores, J.-A., Furota, S., Grunert, P., Hodell, D., Jimenez-Espejo, F., Kim, J. K., Krissek, L., Kuroda, J., Li, B., Llave, E., Lofi, J., Lourens, L., Miller, M., Nanayama, F., Nishida, N., Richter, C., Roque, C., Pereira, H., Sanchez Goñi, M. F., Sierro, F. J., Singh, A. D., Sloss, C., Takashimizu, Y., Tzanova, A., Voelker, A., Williams, T., and Xuan, C.: Onset of Mediterranean outflow into the North Atlantic, Science, 344, 1244-1250, 10.1126/science.1251306, 2014.

Holtvoeth, J., Wagner, T., and Schubert, C. J.: Organic matter in river-influenced continental margin sediments: The land-ocean and climate linkage at the Late Quaternary Congo fan (ODP Site 1075), Geochemistry, Geophysics, Geosystems, 4, 1109, doi:1110.1029/2003GC000590, 2003.

Hughes, J.: Crystallinity of kaolin minerals and their weathering sequence in some soils from Nigeria, Brazil and Colombia, Geoderma, 24, 317-325, 1980.

Ibrahim, K., and Hall, A.: The authigenic zeolites of the Aritayn Volcaniclastic Formation, north-east Jordan, Mineralium Deposita, 31, 514-522, 10.1007/BF00196131, 1996.

Jennerjahn, T., Knoppers, B., Souza, W., Carvalho, C., Mollenhauer, G., Hübner, M., and Ittekkot, V.: The tropical Brazilian continental margin, Carbon and Nutrient Fluxes in Continental Margins, A global synthesis, Berlin: Springer Verlag Heidelberg, 427-436, 2010.

Jonkers, L., Prins, M. A., Brummer, G. J., Konert, M., and Lougheed, B. C.: Experimental insights into laser diffraction particle sizing of fine-grained sediments for use in palaeoceanography, Sedimentology, 56, 2192-2206, 2009.

Kaboth, S., Boer, B., Bahr, A., Zeeden, C., and Lourens, L. J.: Mediterranean Outflow Water dynamics during the past ~570 kyr: Regional and global implications, Paleoceanography, 634–647, 2017.

Kano, A., Ferdelman, T. G., Williams, T., Henriet, J.-P., Ishikawa, T., Kawagoe, N., Takashima, C., Kakizaki, Y., Abe, K., and Sakai, S.: Age constraints on the origin and growth history of a deep-water coral mound in the northeast Atlantic drilled during Integrated Ocean Drilling Program Expedition 307, Geology, 35, 1051-1054, 2007.

Kiriakoulakis, K., Fisher, E., Wolff, G. A., Freiwald, A., Grehan, A., and Roberts, J. M.: Lipids and nitrogen isotopes of two deep-water corals from the North-East Atlantic: initial results and implications for their nutrition, in: Cold-water Corals and Ecosystems, edited by: Freiwald, A., and Roberts, J. M., Springer, Erlangen, 715-729, 2005.

Kroopnick, P.: The distribution of ^{13}C of ΣCO_2 in the world oceans, Deep Sea Research Part A. Oceanographic Research Papers, 32, 57-84, 1985.

Lessa, D. V., Santos, T. P., Venancio, I. M., Santarosa, A. C. A., dos Santos Junior, E. C., Toledo, F. A., Costa, K. B., and Albuquerque, A. L. S.: Eccentricity-induced expansions of Brazilian coastal upwelling zones, Global and Planetary Change, 179, 33-42, 2019.

Lippold, J., Pöppelmeier, F., Süfke, F., Gutjahr, M., Goepfert, T. J., Blaser, P., Friedrich, O., Link, J. M., Wacker, L., Rheinberger, S., and Jaccard, S. L.: Constraining the variability of the Atlantic Meridional Overturning Circulation during the Holocene, Geophysical Research Letters, 46, 11338-11346, 10.1029/2019gl084988, 2019.

Lisiecki, L. E., and Raymo, M. E.: A Pliocene-Pleistocene stack of 57 globally distributed benthic delta O-18 records, Paleoceanography, 20, PA1003, 2005.

Lunden, J. J., McNicholl, C. G., Sears, C. R., Morrison, C. L., and Cordes, E. E.: Acute survivorship of the deep-sea coral Lophelia pertusa from the Gulf of Mexico under acidification, warming, and deoxygenation, Frontiers in Marine Science, 1, 78, 2014.

https://doi.org/10.5194/bg-2020-206
Preprint. Discussion started: 30 June 2020

Magill, C. R., Ausín, B., Wenk, P., McIntyre, C., Skinner, L., Martínez-García, A., Hodell, D. A., Haug, G. H., Kenney, W., and Eglinton, T. I.: Transient hydrodynamic effects influence organic carbon signatures in marine sediments, Nature communications, 9, 4690, 2018.

Maier, C., Watremez, P., Taviani, M., Weinbauer, M., and Gattuso, J.: Calcification rates and the effect of ocean acidification on Mediterranean cold-water corals, Proceedings of the Royal Society B: Biological Sciences, 279, 1716-1723, 2012.

Mangini, A., Godoy, J., Godoy, M., Kowsmann, R., Santos, G., Ruckelshausen, M., Schroeder-Ritzrau, A., and Wacker, L.: Deep sea corals off Brazil verify a poorly ventilated Southern Pacific Ocean during H2, H1 and the Younger Dryas, Earth and Planetary Science Letters, 293, 269-276, 2010.

Marchitto, T., Curry, W., Lynch-Stieglitz, J., Bryan, S., Cobb, K., and Lund, D.: Improved oxygen isotope temperature calibrations for cosmopolitan benthic foraminifera, Geochimica et Cosmochimica Acta, 130, 1-11, 2014.

Marengo, J., Liebmann, B., Grimm, A., Misra, V., Silva Dias, P., Cavalcanti, I., Carvalho, L., Berbery, E., Ambrizzi, T., and Vera, C.: Recent developments on the South American monsoon system, International Journal of Climatology, 32, 1-21, 2012.

McCave, I. N., Manighetti, B., and Robinson, S. G.: Sortable silt and fine sediment size/composition slicing: parameters for palaeocurrent speed and palaeoceanography., Paleoceanography, 10, 593-610, 1995.

McManus, J. F., Francois, R., Gherardi, J.-M., Keigwin, L. D., and Brown-Leger, S.: Collapse and rapid resumption of Atlantic meridional circulation linked to deglacial climate changes, Nature, 428, 834-837, 10.1038/nature02494, 2004.

Mémery, L., Arhan, M., Álvarez-Salgado, X. A., Messias, M.-J., Mercier, H., Castro, C. G., and Ríos, A. F.: The water masses along the western boundary of the south and equatorial Atlantic, Progress in Oceanography, 47, 69-98, 2000.

Meunier, A., and Velde, B.: Biotite Weathering in Granites of Western France, in: Developments in Sedimentology, edited by: Mortland, M. M., and Farmer, V. C., Elsevier, 405-413, 1979.

Meyers, S.: Astrochron: An R package for astrochronology, Available at http: org/web/packages/astrochron/index.html, 2014.

Mienis, F., De Stigter, H., White, M., Duineveld, G., De Haas, H., and Van Weering, T.: Hydrodynamic controls on cold-water coral growth and carbonate-mound development at the SW and SE Rockall Trough Margin, NE Atlantic Ocean, Deep Sea Research Part I: Oceanographic Research Papers, 54, 1655-1674, 2007.

Mienis, F., Bouma, T., Witbaard, R., Van Oevelen, D., and Duineveld, G.: Experimental assessment of the effects of coldwater coral patches on water flow, Marine Ecology Progress Series, 609, 101-117, 2019.

Miramontes, E., Penven, P., Fierens, R., Droz, L., Toucanne, S., Jorry, S. J., Jouet, G., Pastor, L., Silva Jacinto, R., Gaillot, A., Giraudeau, J., and Raisson, F.: The influence of bottom currents on the Zambezi Valley morphology (Mozambique Channel, SW Indian Ocean): In situ current observations and hydrodynamic modelling, Marine Geology, 410, 42-55, https://doi.org/10.1016/j.margeo.2019.01.002, 2019.

Mueller, C., Larsson, A., Veuger, B., Middelburg, J., and Van Oevelen, D.: Opportunistic feeding on various organic food sources by the cold-water coral *Lophelia pertusa*, Biogeosciences, 11, 123, 2014.

Muñoz, A., Cristobo, J., Rios, P., Druet, M., Polonio, V., Uchupi, E., Acosta, J., and Group, A.: Sediment drifts and cold-water coral reefs in the Patagonian upper and middle continental slope, Marine and Petroleum Geology, 36, 70-82, 2012.

Pahnke, K., and Zahn, R.: Southern hemisphere water mass conversion linked with North Atlantic climate variability, Science, 307, 1741-1746, 2005.

Pahnke, K., Goldstein, S. L., and Hemming, S. R.: Abrupt changes in Antarctic Intermediate Water circulation over the past 25,000 years, Nature Geosci, 1, 870-874, 2008.

Poggemann, D.-W., Hathorne, E. C., Nürnberg, D., Frank, M., Bruhn, I., Reißig, S., and Bahr, A.: Rapid deglacial injection of nutrients into the tropical Atlantic via Antarctic Intermediate Water, Earth and Planetary Science Letters, 463, 118-126, 2017.

Raddatz, J., Rüggeberg, A., Margreth, S., Dullo, W.-C., and Expedition, I.: Paleoenvironmental reconstruction of Challenger Mound initiation in the Porcupine Seabight, NE Atlantic, Marine Geology, 282, 79-90, 2011.

Raddatz, J., Rüggeberg, A., Liebetrau, V., Foubert, A., Hathorne, E. C., Fietzke, J., Eisenhauer, A., and Dullo, W.-C.: Environmental boundary conditions of cold-water coral mound growth over the last 3 million years in the Porcupine Seabight, Northeast Atlantic, Deep Sea Research Part II: Topical Studies in Oceanography, 99, 227-236, 2014.

Raddatz, J., Liebetrau, V., Trotter, J., Rüggeberg, A., Flögel, S., Dullo, W. C., Eisenhauer, A., Voigt, S., and McCulloch, M.: Environmental constraints on Holocene cold-water coral reef growth off Norway: Insights from a multiproxy approach, Paleoceanography, 31, 1350-1367, 2016.

Raddatz, J., and Rüggeberg, A.: Constraining past environmental changes of cold-water coral mounds with geochemical proxies in corals and foraminifera, The Depositional Record, 2019.

https://doi.org/10.5194/bg-2020-206
Preprint. Discussion started: 30 June 2020

Raddatz, J., Titschack, J., Frank, N., Freiwald, A., Conforti, A., Osborne, A., Skornitzke, S., Stiller, W., Rüggeberg, A., Voigt, S., Albuquerque, A., Vertino, A., Schröder-Ritzrau, A., and Bahr, A.: *Solenosmilia variabilis*-bearing cold-water mounds off Brazil, doi: 10.1007/s00338-019-01882-w, 2020.

Rebesco, M., Hernández-Molina, F. J., Van Rooij, D., and Wåhlin, A.: Contourites and associated sediments controlled by deep-water circulation processes: State-of-the-art and future considerations, Marine Geology, 352, 111-154, http://dx.doi.org/10.1016/j.margeo.2014.03.011, 2014.

Roberts, J. M., and Cairns, S. D.: Cold-water corals in a changing ocean, Current Opinion in Environmental Sustainability, 7, 118-126, https://doi.org/10.1016/j.cosust.2014.01.004, 2014.

Rohling, E., Foster, G. L., Grant, K., Marino, G., Roberts, A., Tamisiea, M. E., and Williams, F.: Sea-level and deep-sea-temperature variability over the past 5.3 million years, Nature, 508, 477-482, 2014.

Roughan, M., and Middleton, J. H.: A comparison of observed upwelling mechanisms off the east coast of Australia, Continental Shelf Research, 22, 2551-2572, 2002.

Ruckelshausen, M.: Cold-water corals: A paleoceanographic archive; Tracing past ocean circulation changes in the mid-depth subtropical western South Atlantic off Brazil for the last 40 ka BP, PhD, Heidelberg University, 215 pp., 2013.

Rüggeberg, A., Dorschel, B., Dullo, W.-C., and Hebbeln, D.: Sedimentary patterns in the vicinity of a carbonate mound in the Hovland Mound Province, northern Porcupine Seabight, in: Cold-water corals and ecosystems, Springer, 87-112, 2005.

Rüggeberg, A., Flögel, S., Dullo, W. C., Raddatz, J., and Liebetrau, V.: Paleoseawater density reconstruction and its implication for cold-water coral carbonate mounds in the northeast Atlantic through time, Paleoceanography, 31, 365-379, 2016.

Skornitzke, S., Raddatz, J., Bahr, A., Pahn, G., Kauczor, H.-U., and Stiller, W.: Experimental application of an automated alignment correction algorithm for geological CT imaging: phantom study and application to sediment cores from cold-water coral mounds, European radiology experimental, 3, 12, 2019.

Soetaert, K., Mohn, C., Rengstorf, A., Grehan, A., and Van Oevelen, D.: Ecosystem engineering creates a direct nutritional link between 600-m deep cold-water coral mounds and surface productivity, Scientific reports, 6, 35057, 2016.

Stramma, L., and England, M.: On the water masses and mean circulation of the South Atlantic Ocean, Journal of Geophysical Research: Oceans, 104, 20863-20883, 1999.

Stríkis, N. M., Chiessi, C. M., Cruz, F. W., Vuille, M., Cheng, H., Souza Barreto, E. A., Mollenhauer, G., Kasten, S., Karmann, I., and Edwards, R. L.: Timing and structure of Mega-SACZ events during Heinrich Stadial 1, Geophysical Research Letters, 42, 5477-5484, 2015.

Stuut, J.-B. W., Prins, M. A., Schneider, R. R., Weltje, G. J., Jansen, J. F., and Postma, G.: A 300-kyr record of aridity and wind strength in southwestern Africa: inferences from grain-size distributions of sediments on Walvis Ridge, SE Atlantic, Marine Geology, 180, 221-233, 2002.

Sumida, P. Y. G., Yoshinaga, M. Y., Madureira, L. A. S.-P., and Hovland, M.: Seabed pockmarks associated with deepwater corals off SE Brazilian continental slope, Santos Basin, Marine Geology, 207, 159-167, 2004.

Sverdrup, H. U., Johnson, M. W., and Fleming, R. H.: The Oceans: Their physics, chemistry, and general biology, Prentice-Hall New York, 1942.

Thiem, Ø., Ravagnan, E., Fosså, J. H., and Berntsen, J.: Food supply mechanisms for cold-water corals along a continental shelf edge, Journal of Marine Systems, 60, 207-219, 2006.

Thresher, R. E., Tilbrook, B., Fallon, S., Wilson, N. C., and Adkins, J.: Effects of chronic low carbonate saturation levels on the distribution, growth and skeletal chemistry of deep-sea corals and other seamount megabenthos, Marine Ecology Progress Series, 442, 87-99, 2011.

Titschack, J., Thierens, M., Dorschel, B., Schulbert, C., Freiwald, A., Kano, A., Takashima, C., Kawagoe, N., Li, X., and Expedition, I.: Carbonate budget of a cold-water coral mound (Challenger Mound, IODP Exp. 307), Marine Geology, 259, 36-46, 2009.

Titschack, J., Baum, D., De Pol-Holz, R., López Correa, M., Forster, N., Flögel, S., Hebbeln, D., and Freiwald, A.: Aggradation and carbonate accumulation of Holocene Norwegian cold-water coral reefs, Sedimentology, 62, 1873-1898, 10.1111/sed.12206, 2015.

Titschack, J., Fink, H. G., Baum, D., Wienberg, C., Hebbeln, D., and Freiwald, A.: Mediterranean cold-water corals–an important regional carbonate factory?, The Depositional Record, 2, 74-96, 2016.

Turnewitsch, R., Reyss, J.-L., Chapman, D. C., Thomson, J., and Lampitt, R. S.: Evidence for a sedimentary fingerprint of an asymmetric flow field surrounding a short seamount, Earth and Planetary Science Letters, 222, 1023-1036, http://dx.doi.org/10.1016/j.epsl.2004.03.042, 2004.

van Oevelen, D., Mueller, C. E., Lundälv, T., and Middelburg, J. J.: Food selectivity and processing by the cold-water coral Lophelia pertusa, Biogeosciences, 13, 5789-5798, 2016.

https://doi.org/10.5194/bg-2020-206
Preprint. Discussion started: 30 June 2020

845 Viana, A., and Faugères, J.-C.: Upper slope sand deposits: the example of Campos Basin, a latest Pleistocene-Holocene record of the interaction between alongslope and downslope currents, Geological Society, London, Special Publications, 129, 287-316, 1998.

Viana, A., Faugères, J., Kowsmann, R., Lima, J., Caddah, L., and Rizzo, J.: Hydrology, morphology and sedimentology of the Campos continental margin, offshore Brazil, Sedimentary Geology, 115, 133-157, 1998.

850 Viana, A. R.: Seismic expression of shallow-to deep-water contourites along the south-eastern Brazilian margin, Marine Geophysical Researches, 22, 509-521, 2001.

Waelbroeck, C., Labeyrie, L., Michel, E., Duplessy, J. C., McManus, J. F., Lambeck, K., Balbon, E., and Labracherie, M.: Sea-level and deep water temperature changes derived from benthic foraminifera isotopic records, Quaternary Science Reviews, 21, 295-305, 2002.

855 Waelbroeck, C., Pichat, S., Bohm, E., Lougheed, B. C., Faranda, D., Vrac, M., Missiaen, L., Vazquez Riveiros, N., Burckel, P., and Lippold, J.: Relative timing of precipitation and ocean circulation changes in the western equatorial Atlantic over the last 45 kyr, Climate of the Past, 14, 1315-1330, 2018.

Wang, X., Auler, A. S., Edwards, R. L., Cheng, H., Cristalli, P. S., Smart, P. L., Richards, D. A., and Shen, C.-C.: Wet periods in northeastern Brazil over the past 210 kyr linked to distant climate anomalies, Nature, 432, 740-743,
860 10.1038/nature03067, 2004.

Weaver, R.: Quartz presence in relationship to gibbsite stability in some highly weathered soils of Brazil, Clays and Clay Minerals, 23, 431-436, 1975.

White, M., Wolff, G. A., Lundälv, T., Guihen, D., Kiriakoulakis, K., Lavaleye, M., and Duineveld, G.: Cold-water coral ecosystem (Tisler Reef, Norwegian Shelf) may be a hotspot for carbon cycling, Marine Ecology Progress Series,
865 465, 11-23, 2012.

Wienberg, C., and Titschack, J.: Framework-forming scleractinian cold-water corals through space and time: a late Quaternary North Atlantic perspective, in: Marine Animal Forests: The Ecology of Benthic Biodiversity Hotspots, edited by: Rossi S, Bramanti L, Gori A, and C, O., Springer International Publishing, Cham, 699-732, 2017.

Wienberg, C., Titschack, J., Freiwald, A., Frank, N., Lundälv, T., Taviani, M., Beuck, L., Schröder-Ritzrau, A.,
870 Krengel, T., and Hebbeln, D.: The giant Mauritanian cold-water coral mound province: Oxygen control on coral mound formation, Quaternary Science Reviews, 185, 135-152, 2018.

Wilson, M.: A study of weathering in a soil derived from a biotite-hornblende rock: I. Weathering of biotite, Clay Minerals, 8, 291-303, 1970.

Zahn, R., Winn, K., and Sarnthein, J. M.: Benthic foraminiferal $d^{13}C$ and accumulation rates of organic carbon:
875 *Uvigernina peregrina* group and *Cibicidoides wuellerstorfi*, Paleoceanography, 1, 27-42, 1986.